

General Disclaimer

One or more of the Following Statements may affect this Document

- This document has been reproduced from the best copy furnished by the organizational source. It is being released in the interest of making available as much information as possible.
- This document may contain data, which exceeds the sheet parameters. It was furnished in this condition by the organizational source and is the best copy available.
- This document may contain tone-on-tone or color graphs, charts and/or pictures, which have been reproduced in black and white.
- This document is paginated as submitted by the original source.
- Portions of this document are not fully legible due to the historical nature of some of the material. However, it is the best reproduction available from the original submission.

**NASA TECHNICAL
MEMORANDUM**

NASA TM-73,235

NASA TM-73,235

(NASA-TM-X-73235) INTERIOR AND EXTERIOR
FUSELAGE NOISE MEASURED ON NASA'S C-8A
AUGMENTOR WING JET-STOL RESEARCH AIRCRAFT
(NASA) 50 p HC A03/MF A01 CSCL 20A

N77-24137

**G3/07 Unclass
30347**

**INTERIOR AND EXTERIOR FUSELAGE NOISE MEASURED ON
NASA'S C-8A AUGMENTOR WING JET-STOL RESEARCH AIRCRAFT**

Michael D. Shovlin

**Ames Research Center
Moffett Field, California 94035**

April 1977

**JUN 1977
RECEIVED
NASA STI FACILITY
INPUT BRANCH**

1. Report No. NASA TM-73,235		2. Government Accession No.		3. Recipient's Catalog No.	
4. Title and Subtitle INTERIOR AND EXTERIOR FUSELAGE NOISE MEASURED ON NASA'S C-8A AUGMENTOR WING JET-STOL RESEARCH AIRCRAFT				5. Report Date	
				6. Performing Organization Code	
7. Author(s) Michael D. Shovlin				8. Performing Organization Report No. A-7012	
9. Performing Organization Name and Address Ames Research Center, NASA Moffett Field, Calif., 94035				10. Work Unit No. 769-02-02	
				11. Contract or Grant No.	
12. Sponsoring Agency Name and Address National Aeronautics and Space Administration Washington, D. C. 20456				13. Type of Report and Period Covered Technical Memorandum	
				14. Sponsoring Agency Code	
15. Supplementary Notes					
16. Abstract Interior and exterior fuselage noise levels were measured on NASA's C-8A Augmentor Wing Jet-STOL Research Aircraft in order to provide design information for the Quiet Short-Haul Research Aircraft (QSRA), which will use a modified C-8A fuselage. The noise field was mapped by 11 microphones located internally and externally in three areas: mid-fuselage, aft fuselage, and on the flight deck. Noise levels were recorded at four power settings varying from takeoff to flight idle and were plotted in one-third octave band spectra. The overall sound pressure levels of the external noise field were compared to previous tests and found to correlate well with engine primary thrust levels. Fuselage values were 145 ± 3 dB over the aircraft's normal STOL operating range.					
17. Key Words (Suggested by Author(s)) Aircraft noise Powered lift Fuselage noise levels C8-A augmentor wing			18. Distribution Statement Unlimited STAR Category - 07		
19. Security Classif. (of this report) Unclassified		20. Security Classif. (of this page) Unclassified		21. No. of Pages 49	
				22. Price* \$3.75	

INTERIOR AND EXTERIOR FUSELAGE NOISE

MEASURED ON NASA'S C-8A AUGMENTOR WING JET-STOL RESEARCH AIRCRAFT

Michael D. Shovlin

Ames Research Center

Moffett Field, California 94035

SUMMARY

Interior and exterior fuselage noise levels were measured on NASA's C-8A Augmentor Wing Jet-STOL Research Aircraft in order to provide design information for the Quiet Short-Haul Research Aircraft (QSRA), which will use a modified C-8A fuselage. The noise field was mapped by 11 microphones located internally and externally in three areas: mid-fuselage, aft fuselage, and on the flight deck. Noise levels were recorded at four power settings varying from takeoff to flight idle and were plotted in one-third octave band spectra. The overall sound pressure levels of the external noise field were compared to previous tests and found to correlate well with engine primary thrust levels. Fuselage values were 145 ± 3 dB over the aircraft's normal STOL operating range.

INTRODUCTION

Shortly after NASA's C-8A Buffalo Augmentor Wing Jet-STOL Research Aircraft (AWJSRA) became operational in 1972, a number of fatigue cracks were noticed in the mid and aft fuselage areas. After an initial series of cracks, fatigue damage occurrence dropped to a level where an occasional crack was noted and repaired during post flight inspection. This fatigue damage was attributed to the high structural-acoustic loads generated by the propulsive-lift system and jet exhaust on a fuselage that had originally been designed by de Havilland, Ltd. for use in the C-8A turboprop transport aircraft.

A second prototype C-8A Buffalo fuselage is being used in the Quiet Short-Haul Research Aircraft (QSRA), which is currently being designed by the Boeing Commercial Airplane Company, and which will be used to perform research in the hybrid upper surface blown propulsive-lift concept. Although the QSRA will be an exceptionally quiet airplane, the propulsive-lift system exposes the aircraft structure to an extremely harsh environment, particularly on the sides of the fuselage aft of the wing trailing edge. Because fatigue damage had occurred in AWJSRA's C-8A fuselage which was attributed to structural-acoustic loads, there is concern that the QSRA's C-8A fuselage will also be subject to fatigue damage resulting from a similar environment. The fatigue damage that occurred in the AWJSRA program was more of an annoyance than a safety hazard and it is felt that if the QSRA's environment were the same or less severe than that of the AWJSRA then no costly modifications would be required to its fuselage. Conversely, if the environment proves to be substantially more severe, then modification might be required to the QSRA fuselage to assure flight safety. Boeing predicted the sonic environment of the QSRA. Although the AWJSRA had a history of previous fatigue damage, the structural-acoustic environment had not been measured or predicted prior to the current test.

The present study presents the results of a series of noise measurements made simultaneously inside and outside the AWJSRA fuselage in three areas: mid fuselage in the area of maximum fatigue damage; aft fuselage section where QSRA sonic environment is expected to be the most severe; and the flight deck at the pilot's station.

Contributions by Paul T. Soderman in support of the acoustic analysis and of Vard B. Holland and Bruce Lilley in support of the aircraft operations are gratefully acknowledged.

MODIFIED C-8A AIRCRAFT

The C-8A Buffalo Augmentor Wing Jet-STOL Research Aircraft is a modified version of a high-wing, T-tail turboprop military transport manufactured by de Havilland, Ltd. of Canada, and modified jointly by the Boeing Commercial Airplane Company and de Havilland. It is used to study the design and operational characteristics of jet-STOL aircraft using split-flow turbofan engines to provide both direct propulsive lift and augmentor wing lift. A description of the modified C-8A is given in Table 1 and in figure 1. Additional details of the flight and research characteristics of the aircraft are given in reference 1 and 2. Several features of its powered-lift and propulsion system are briefly described below, while a more complete description of all the aircraft's design features is given in reference 3.

Propulsion System

Two Rolls Royce Spey MK 801-SF split flow engines, one mounted in each nacelle (figure 1), provide thrust for the aircraft as well as air for the augmentation system. These are hybrid engines built by Rolls Royce specifically for this application with a 0.6 bypass ratio and a maximum cold flow pressure ratio of 2.5. The engine hot flow is discharged into a Pegasus trouser piece and out through two vectorable

conical nozzles (figure 2), while the cold flow is collected and discharged through two 0.33 m diameter ducts located at the top of the engine which supply the distribution system described below. The hot and cold flow engine thrust split is shown on figure 3 where the cold (bypass air) thrust shown is the isentropic thrust at the engine offtake.

Air Distribution System

The distribution system directs the engine cold flow air to the augmentor nozzles, to the aileron nozzles, and to the fuselage boundary layer blowing nozzles, as shown in figures 4 and 5.

A crossover ducting system directs approximately 64 percent of the bypass mass flow along the front of the wing and across the interior of the fuselage to the augmentor and aileron nozzles on the opposite side of the airplane and to half of the fuselage boundary layer blowing nozzles; the remaining 36 percent of the flow is directed back to the augmentor nozzles on the same side as the engine. Of the 64 percent of the engine mass flow carried by the crossover ducting system, approximately 7 percent is used for fuselage blowing, 44 percent by the augmentor nozzles, and the remaining 13 percent by the aileron boundary layer control nozzles (figures 5 and 6). For reference, the physical characteristics of the mass flow at the takeoff power-setting are 36 kg/sec per engine at 132°C with a pressure ratio of 2.5.

ACOUSTIC TEST

The aircraft near field noise levels were measured at the Ames Research Center's X-14 static test site which is located away from the Center's main buildings. Figure 7 shows the C-8A parked on one of the heavy thrust pads of the site, where the nearest building, a trailer, was approximately 35 m away and in a line slightly forward of the instrumented quadrant.

The left side of the aircraft was chosen for the test measurements because the fuselage interior on that side was essentially an unmodified C-8A configuration, while the right side of the fuselage forward of the door has additional hydraulic and test equipment installed on the fuselage structure. In addition to being more accessible, the left side appears to have sustained a higher level of fatigue damage, possibly because the new systems on the right side add considerable stiffness and increased mass.

The interior was acoustically isolated from the exterior field as much as possible; the fuselage air vents and blowout panels were stuffed with polyurethane foam; the blowout area was covered with a sheet of 1.25 cm exterior plywood. Resonance effects in the fuselage cavity were minimized by a series of equipment racks running down the center of the fuselage one meter from the flight deck to, with the addition of the noise measuring equipment, within one meter of the door. In addition, the crossover ducts ran across the center of the fuselage and a large number of aircraft systems were ceiling or side mounted, giving large numbers of random surfaces throughout the fuselage interior. Finally, all of the fuselage thermal insulation pads have been removed, resulting in bare aircraft structure with virtually all of the fuselage interior surface acoustically hard.

Equipment and Installation

The noise data was measured with 11 Bruel and Kjaer 1.27 cm (1/2 inch) diameter, type 4133, condenser microphones and recorded on an Ampex FR1300 A multichannel tape recorder. Microphones 7-11 were equipped with wind shield nose cones; however, no appreciable flow was observed over or around them during the test.

The interior microphones (2-6) were mounted on "C" clamp fixtures (see figure 8) which were attached to the aircraft structure by using fiberboard and aluminum pressure pads, assuring a rigid mount at the clamp end. The 0.64 cm (1/4 inch) steel rod end was bent so that a

microphone taped to it would be positioned in the center of a panel area, about 1-2 cm from the skin surface. Vibration of the rod end with its attached microphone was minimized by running tape from it to different surrounding aircraft frames.

In the mid-fuselage area, three microphones (7-9) were used to measure the external field (figure 9). These microphones were mounted on 1.82 m stands with the diaphragm parallel to the ground and pointing up. (The ground power cables shown in the picture were removed when the engine was started). The three interior microphones (2-4) are shown in figure 9, where 2 and 3 are installed between window frames and 4 is installed on the panel above the frame because of the fire extinguisher location. A portion of the crossover duct can also be seen in the right hand corner of the figure, just above microphone 2. The physical locations of each of the microphones, 2-4 and 7-9, are shown on the sketch of figure 10.

The locations of the aft fuselage microphones (4, 5, 10, and 11) are shown in figures 11 and 12. The left side of the fuselage is somewhat cluttered aft of the door, with safety equipment and a main electrical panel, requiring these microphones to be placed rearward of this area. The microphones were located half way from the floor to the fuselage shoulder and on both sides of the main support frame at the end of the cargo ramp. The external microphones (10-11) were placed outside directly opposite the interior microphones (5-6) and positioned approximately 5 cm from the fuselage skin with the diaphragm parallel to the ground and pointing upwards.

A single microphone (No. 1), was installed on the flight deck, behind the left hand seat 0.91 m above the floor, 12 cm to the left of center of the pilot's seat (see figure 13).

Test Procedure

During the test only the left hand engine was operated. Although this procedure would adequately define the incident field in a normal aircraft, the augmentor jet flap concept is unique in that approximately half of the augmentor flap flow is provided by the opposite side engine. The impact of the operating procedure on the data will be discussed in a later section.

The engine was started and allowed to run at ground idle until its operating parameters stabilized; at that time data was taken at the following engine power settings: flight idle, normal takeoff, maximum continuous, flight idle, and 80 percent. A detailed list of engine operating parameters is given in table II. The engine was stabilized at each power setting and then data was recorded for approximately one minute. The slight upward shift of the flight idle speed for the second point (table II) is due to the increased temperature of the engine and nacelle at the end of the test.

The aircraft flaps and hot nozzles were set at their minimum deflected positions of 5.6 and 6 degrees below the horizontal respectively. These angle settings were maintained for the test series in order to prevent engine operating problems due to reingestion and to limit ground reflection as much as possible.

While the acoustic data was being recorded the atmospheric conditions were fairly ideal with a temperature of 22.2°C and a relative humidity of 46 percent, a barometric pressure of 29.98 inches of mercury and winds less than 2 m/sec.

PRESENTATION OF DATA

The results of the acoustic measurements of the external field (microphones 7-11) are given in figures 14-18 as one-third octave band

frequency spectra. The one-third octave band analysis was computed with a Bruel and Kjaer Real Time Analyzer with all data integrated over a period of 30 seconds or longer. There is some clipping at the higher power settings in all of the external field data; the amount varies with microphone location with the least amount at microphone 9.

The results of the internal measurements (microphones 2-6) are given in figures 19-23 as one-third octave spectral data. There was a slight amount of clipping at the mid-fuselage locations during high power settings. Microphone 2, which showed severe clipping, was installed using a goose neck, and became detached from its pre-amplifier during the test. In addition, the crossover duct and wing structural transmission paths introduce an undetermined amount of noise and vibration in the vicinity of microphone 2. Because of these factors, care should be taken when interpreting the data presented in these figures.

The one-third octave band spectral data measured on the flight deck is presented in figure 24. Care should also be taken in interpreting this data, as a crew member opened a window on the right side of the aircraft sometime in the later stages of the test.

External Acoustic Field

A prime objective of this study is to define the external fuselage structural-acoustic environment with sufficient accuracy to provide design information that can be used to provide design data for the QSRA-C-8A fuselage with minimum cost impact. The highest accuracy is required in the low and mid-frequency range which has the greatest potential impact on structural damage; the overall sound pressure levels, however, should be representative of the levels experienced in the normal operation.

One Engine Operation: - Only the left side engine was operated during the test, resulting in an accurate representation of the hot thrust, but providing only half of the usual two-engine cold flow. The effect of this reduced cold flow on the level of the fuselage acoustic field is believed to be minimal for several reasons: (a) in previous far field measurements (ref. 4), the dominant noise source was determined to be the primary exhaust system of the Spey engine; (b) in the previous two-engine test, the far field noise levels were shown to correlate well with the hot thrust level, and, (c) the majority of low and mid-fuselage noise is produced by the hot flow, which is accurately represented.

Acoustic Source Characteristics: - The Spey engine hot thrust is directed into a Pegasus trouser piece and out through two conical nozzles, each with an exit diameter of 0.54 m and area of 0.23 m^2 (figure 2). In addition, the correct back pressure on the engine is maintained by use of a "colander plate" inserted in the inlet to the trouser piece, which consists of a plate with four hundred 2.54 cm holes. All of the hot flow that passes through this plate, is split into two streams in the trouser piece, and then is exited through the two conical nozzles. Representative physical characteristics of this hot flow are given in figure 25, where the velocities are for fully expanded flow. Additional information on the hot and cold flow characteristics of this engine are given in references 3, 4, and 5.

The second major source in the external noise field is the augmentor nozzle and flap system which is shown in figures 1, 4, 5, and 26. The augmentor nozzle consists of two nozzles located one above the other, each with a geometric height of 0.533 cm, an effective height of 0.466 cm, and length of 7.15 m.

These nozzles direct the high pressure cold flow into the bi-surface augmentor flap proper, where it is aligned with the center of the diffusing and mixing chamber formed by the upper and lower flap

surface (figure 26). The high velocity (sonic) air from the nozzle is shielded from the flap surfaces by the secondary air induced by the augmentation process in order to minimize losses.

The location of these sources relative to the microphones are shown on figure 27. Assuming a potential core length of about 5-7 nozzle diameters, the jet transition region would be located from 3 to 7 m downstream of the nozzle exit, placing the maximum noise generation area about 3 m from the mid-fuselage, assuring a fairly uniform acoustic field on the area aft of the wing trailing edge.

The data from the present test were extrapolated to the far field using the r-square distance variation and correcting for two-engine operation, resulting in values approximately 6dB above the corresponding true free field level. These data are shown (figure 28) to correlate well with the OASPL vs thrust curve of ref. 4, exhibiting a similar change of OASPL level with hot thrust variation.

Fuselage Sound Pressure Levels

The sound pressure levels (OASPL) are given in table III for each microphone location (7-11) and power setting. The sound pressure levels varied from 145dB at maximum continuous power to 148dB on the aft fuselage at takeoff power.

The normal operating range of the AWJSRA is from a power setting in the neighborhood of 90 percent high pressure compressor speed, N_h , during cruise and ferry missions to a STOL operating range of 93 to 99 percent N_h . In actual practice the lower limit of the STOL operating range is shifted toward the max/continuous power setting due to the ambient temperature usually being higher than that of the standard day during most of the STOL operations (ref. 6). The average value of sound

pressure level on the mid-fuselage during maximum continuous operation (96 percent N_h) was 145dB. From figure 28 it can be seen that the level would be about 3dB higher at takeoff power (99 percent N_h), which agrees with the measured data, and about 3dB lower at the approach power setting (93 percent N_h), yielding an average sound pressure level in the mid-fuselage area of 145±3dB during STOL operations. The sound pressure levels would be slightly lower on the aft fuselage, as the nozzles usually point downwards at the higher power settings and some small effect from forward speed can be expected.

CONCLUDING REMARKS

The internal and external noise levels on the fuselage of the C-8A Augmentor Wing Jet-STOL Research Aircraft were measured to provide design information for the Quiet Short-Haul Research Aircraft, which will use a similar C-8A fuselage. This noise field was mapped by 11 microphones located in the aft and mid-fuselage areas and on the flight deck. Data was recorded at four power settings varying from flight idle to takeoff and plotted in one-third octave band spectra. Measurements were made on the left side of the aircraft with only the left engine operating, however, it is believed that the sound field is adequately represented, particularly at low and mid-frequencies. Previous tests showed that the dominant noise source was the hot exhaust flow of the Rolls Royce Spey 801 SF engine, and measured data from the present test show a similar dependence on hot thrust level. The measured values of the external field varied from 145 to 148dB at the higher power settings. The overall sound pressure level on the fuselage aft of the wing is predicted to be in the range of 145±3dB during normal STOL operations, based on the observed OASPL variation with hot thrust level.

Ames Research Center

National Aeronautics and Space Administration

Moffett Field, California 94035, March 31, 1977

REFERENCES

1. Quigley, Hervey C.; Innis, Robert C.; and Grossmith, Seth: A Flight Investigation of the STOL Characteristics of an Augmented Jet Flap STOL Research Aircraft. NASA TM X-62334, 1974.
2. Vomaske, Richard F.; Innis, Robert C.; Swan, Brian E.; Grossmith, Seth W.: A Flight Investigation of the Stability, Control, and Handling Qualities of an Augmented Jet Flap Aircraft. Proposed NASA TN-D.
3. Ashleman, R. H. and Shavdahl, H.: The Development of an Augmentor Wing Jet STOL Research Aircraft (Modified C-8A). NASA CR-114503, 1972.
4. Conway, John A.: The Development of an Intergral Propulsion System for Jet STOL Flight Research. Paper presented at AGARD Propulsion and Energetics Panel Meeting on V/STOL Propulsion, September 1973.
5. Marrs, C.C.; Harkonen, D. L. and O'Keefe, J. V.: Static Noise Tests on Augmentor Wing Jet STOL Research Aircraft (C-8A Buffalo). NASA CR-137520, 1974.
6. Innis, Robert C.; and Quigley, Hervey C.: Operational Experience with a Powered-Lift STOL Aircraft - Aircraft Safety and Operating Problems. NASA SP-416, 1976.

Table I.- Modified C-8A Aircraft Characteristics

Weights, N

Maximum gross	213,000
Maximum gross (STOL takeoff)	200,000
Maximum gross (STOL landing)	191,000
Operational empty	145,000

Areas, m²

Wing area	80
Wing flap area (including ailerons)	17
Horizontal tail area	21
Vertical tail area	14

Dimensions and General Data

Wing, m	
Span	24
Root chord	3.8
Tip chord	2.3
Mean Aerodynamic chord	3.7
Sweepback at 40 percent chord, rad	0.0
Dihedral, outer wing only, rad	0.09

(Note: Wing taper and dihedral each start 5.4 m from plane of symmetry.)

Aspect ratio	7.2
--------------	-----

Horizontal tail, m

Span	9.7
Root chord	2.5
Mean Aerodynamic chord	1.9
Sweep of leading edge, rad	0.08
Dihedral, rad	0.0
Aspect ratio	4.4

Vertical tail, m

Span	4.1
Root chord	4.2
Mean Aerodynamic chord	3.5
Sweep of leading edge, rad	0.4
Aspect ratio	1.2

Overall height, m	8.8
Overall length (with 4.9 m nose boom), m	28.3

Control Surface Deflections

Flaps	0.1 rad down to 1.26 rad down
Conical nozzles	0.11 to 1.82 rad (down from aft of aircraft)
Ailerons	± 0.3 rad about a $+0.61$ rad max droop angle
Augmentor choke	55 percent choke gap closure at maximum flap deflection

TABLE II. OPERATING PARAMETERS OF THE ROLLS ROYCE SPEY 801

ENGINE DURING THE TEST

Point	Engine Power Setting	High Pressure Compressor Speed, N_h , Percent	Low Pressure Compressor Speed, N_L , Percent	Exhaust Gas Temperature $^{\circ}C$
1	Flight Idle	55.1	27.6	435
2	Max. Continuous	96.0	93.3	515
3	Takeoff	98.5	98.7	550
4	Flight Idle	58.0	28.9	430
5	Low Thrust	80.3	45.6	425

TABLE III. OVERALL SOUND PRESSURE LEVEL OF THE FUSELAGE
EXTERNAL ACOUSTIC FIELD

Engine Setting	Microphone Station*					
	7	8	9	10	11	1
Takeoff	146.3	147.4	147.4	148.3	145.3	113.6
Max. Continuous	145.6	144.8	145.9	143.4	143.	111.9
Flight Idle	111.9	110.9	108.4	103.3	104.3	89.0

* OASPL in dB re 2×10^{-5} N/M²

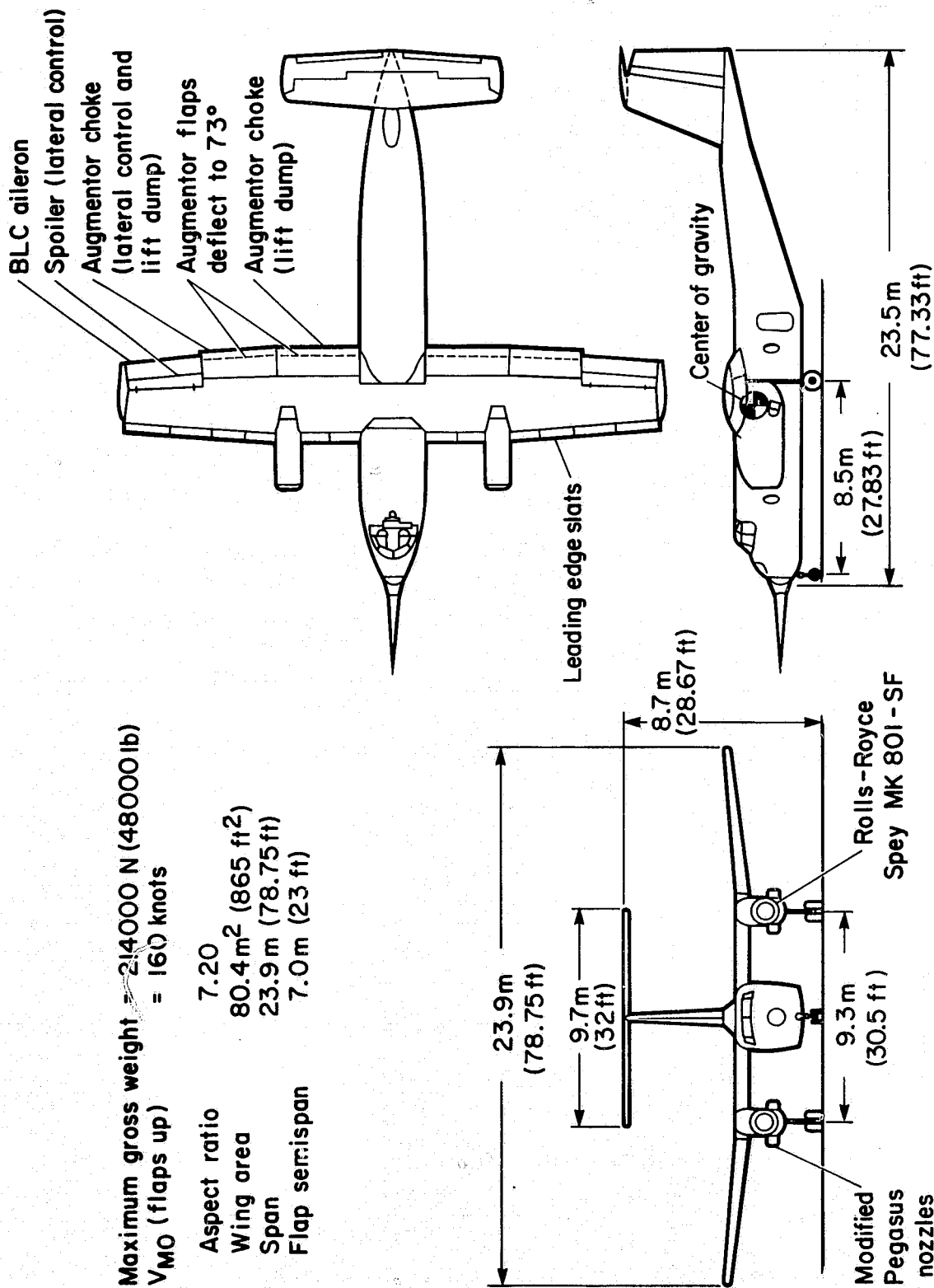


Figure 1.— Three-view drawing of modified C-8A.

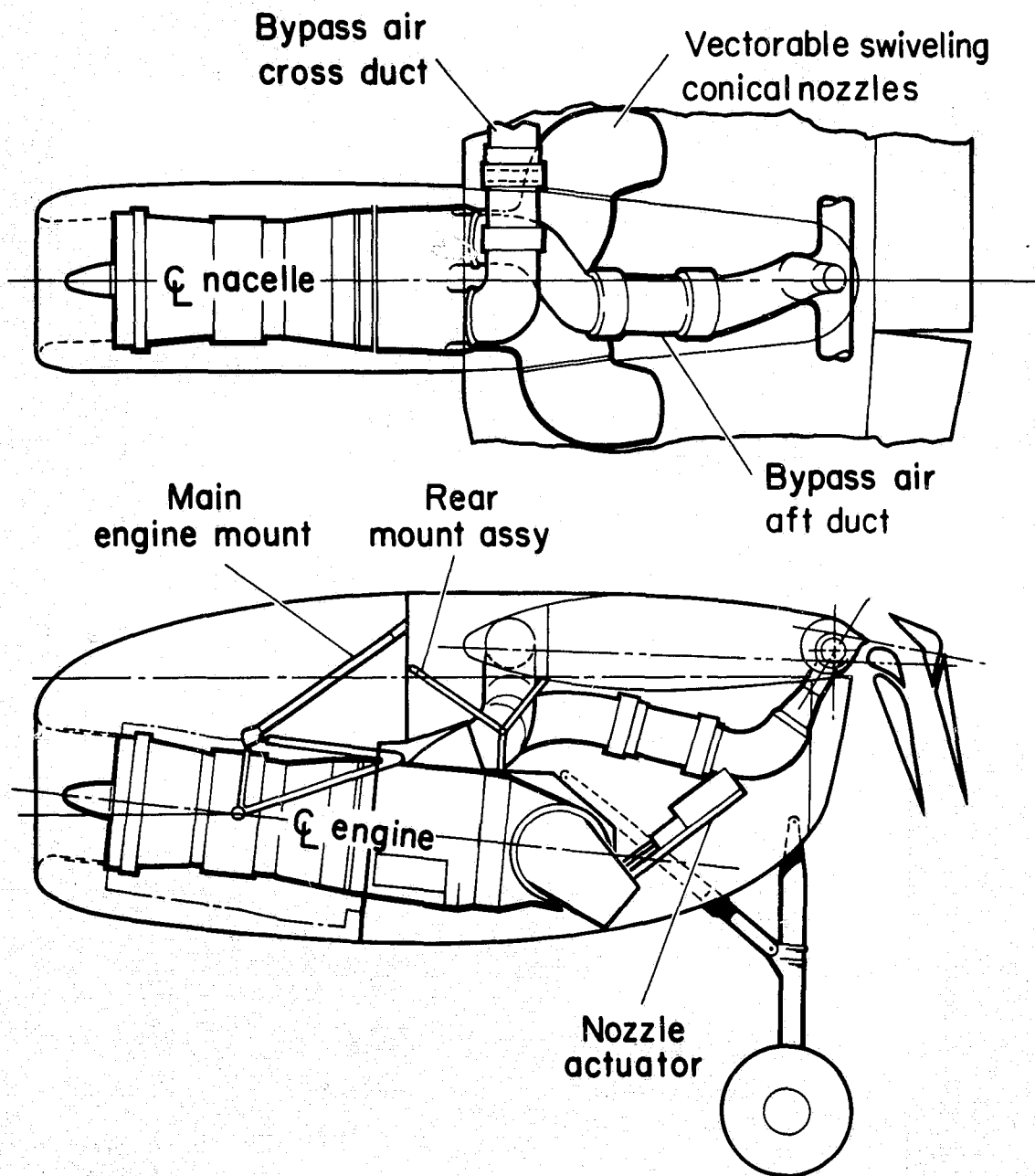


Figure 2.— AWJSRA propulsion system installation.

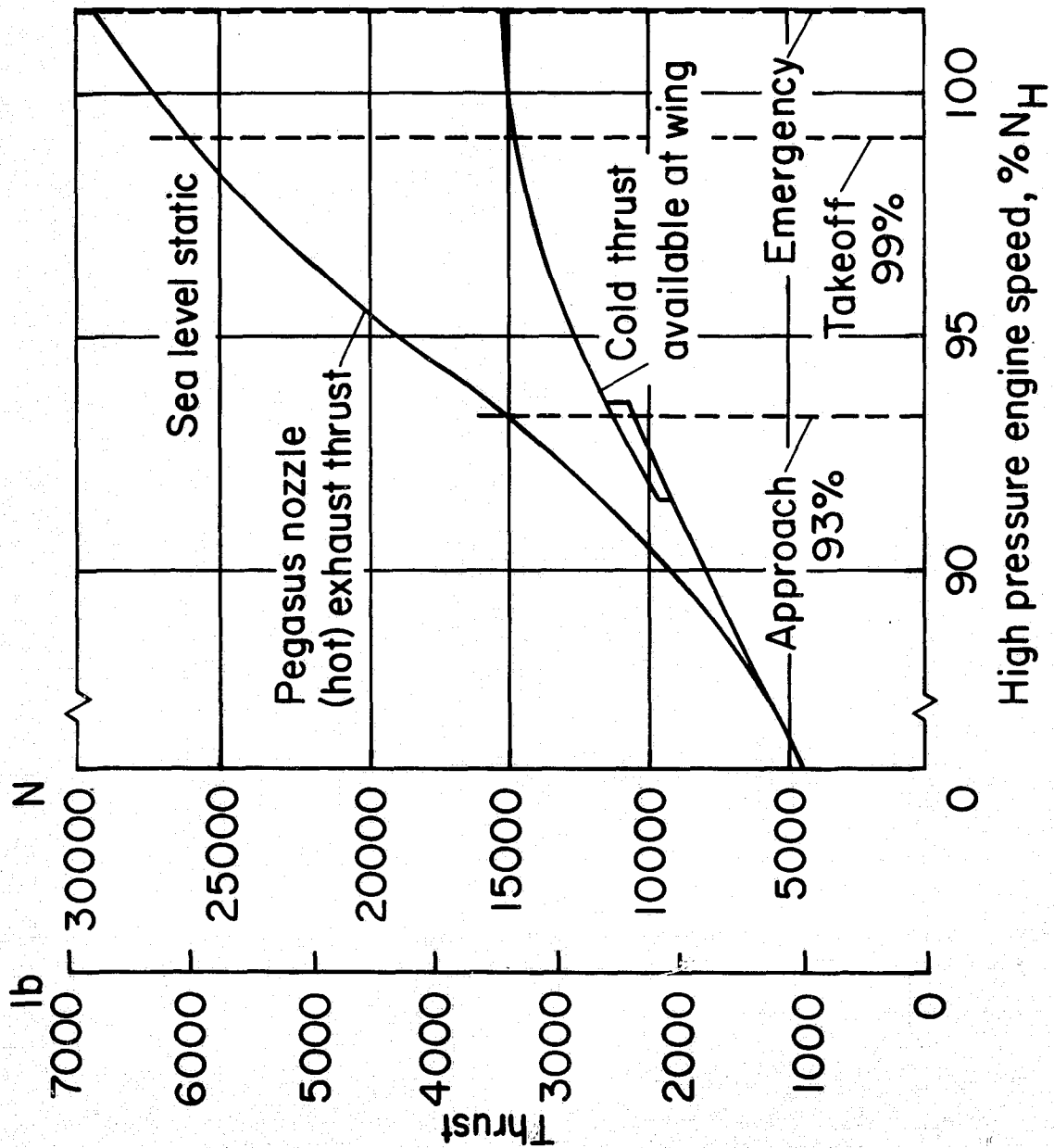


Figure 3.— Rolls Royce Spey 801SF engine thrust.

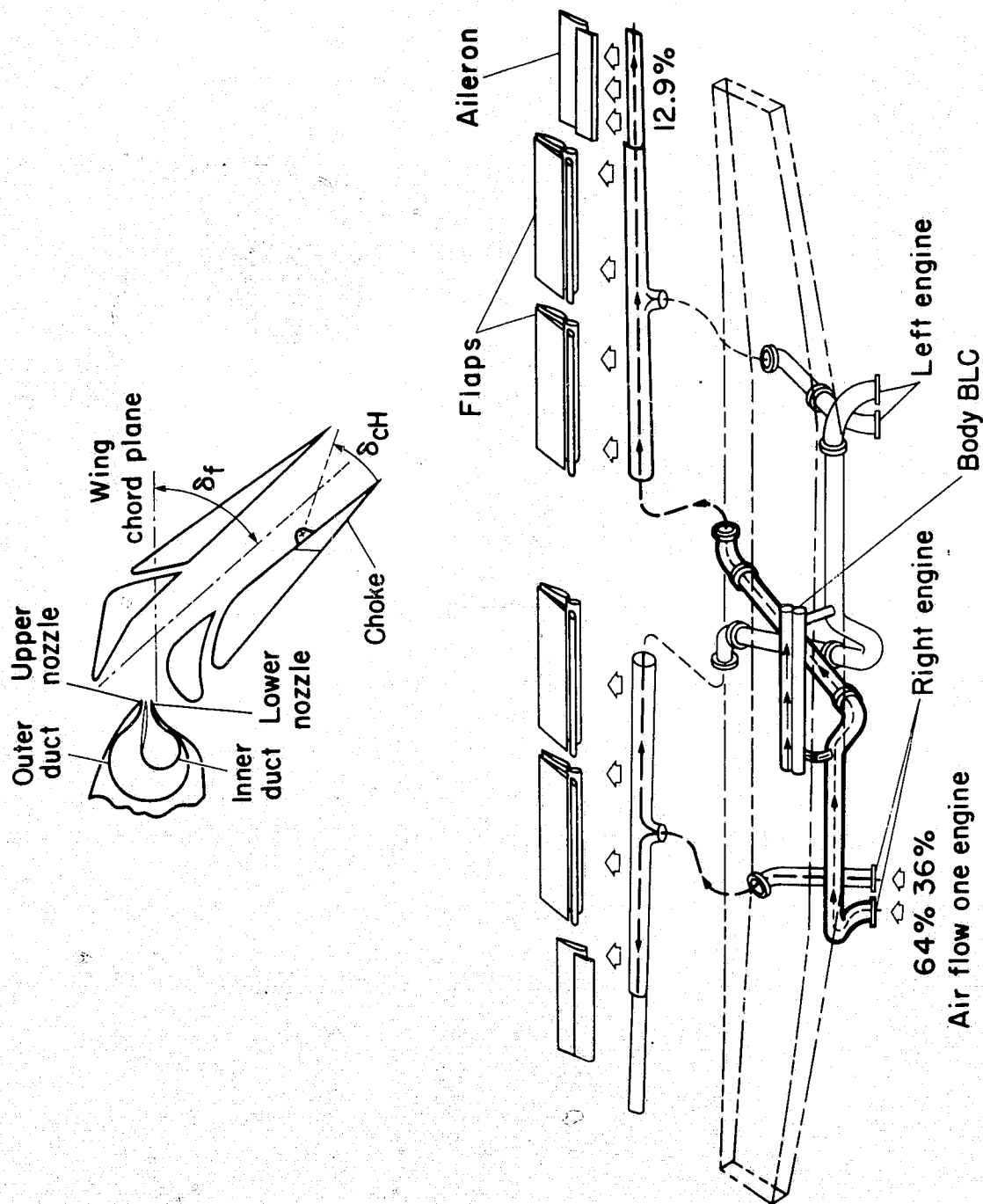


Figure 4.- AMJSRA cold flow air distribution system.

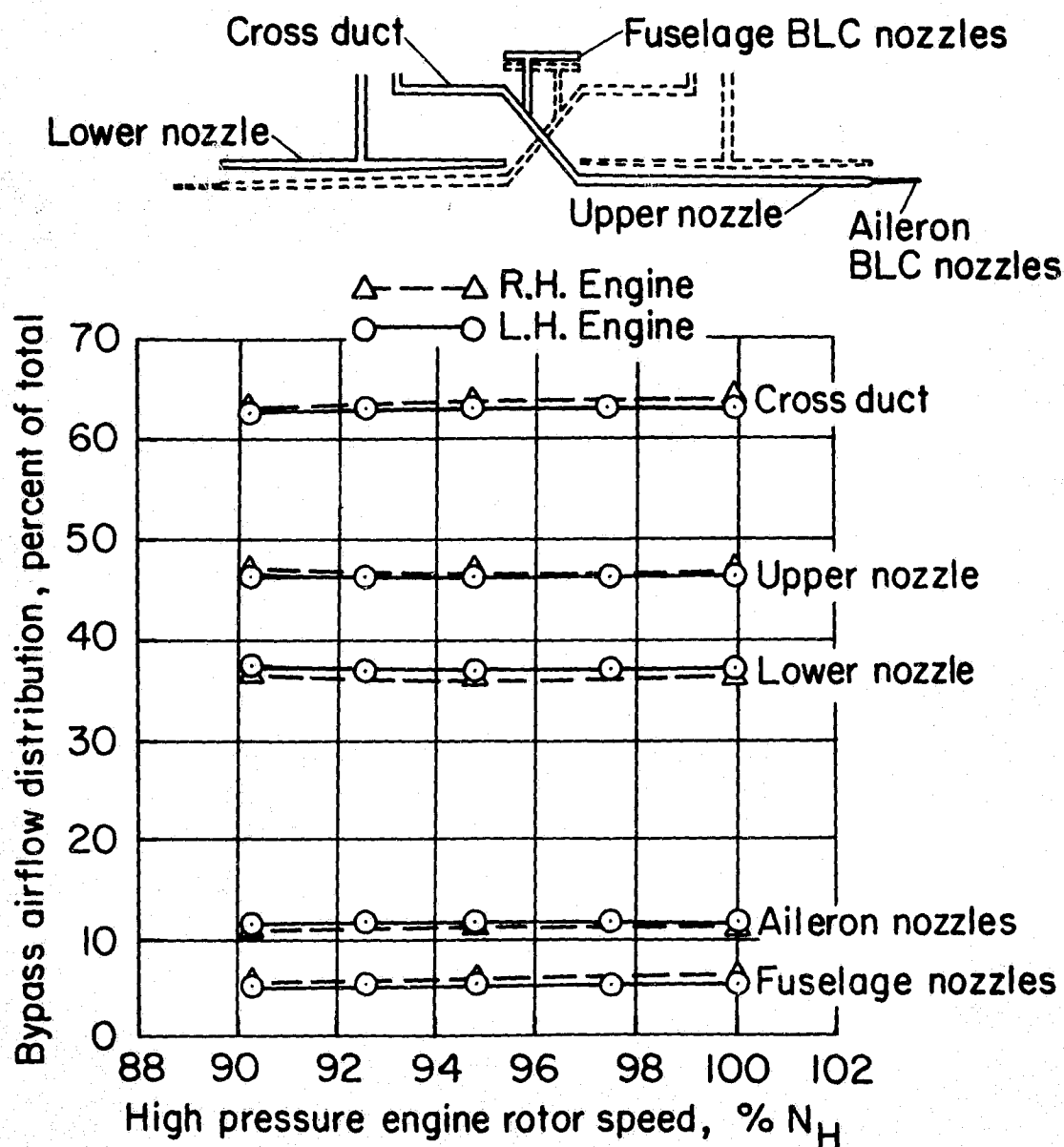


Figure 5.— Bypass flow distribution.

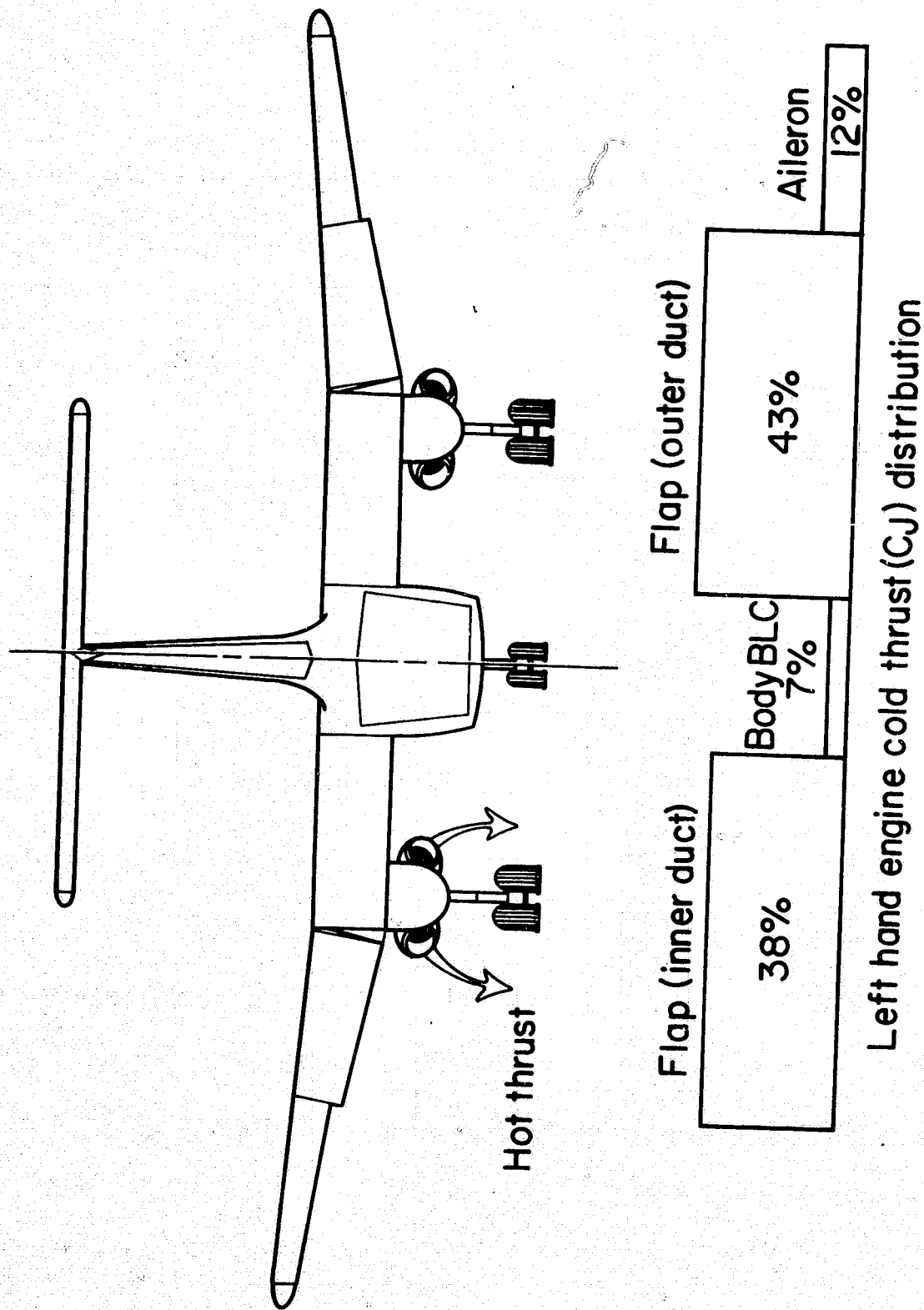


Figure 6.— Left-hand engine cold thrust distribution.



Figure 7.— AWJSRA at Ames Research Center's X-14 test site.



Figure 7.- Concluded.

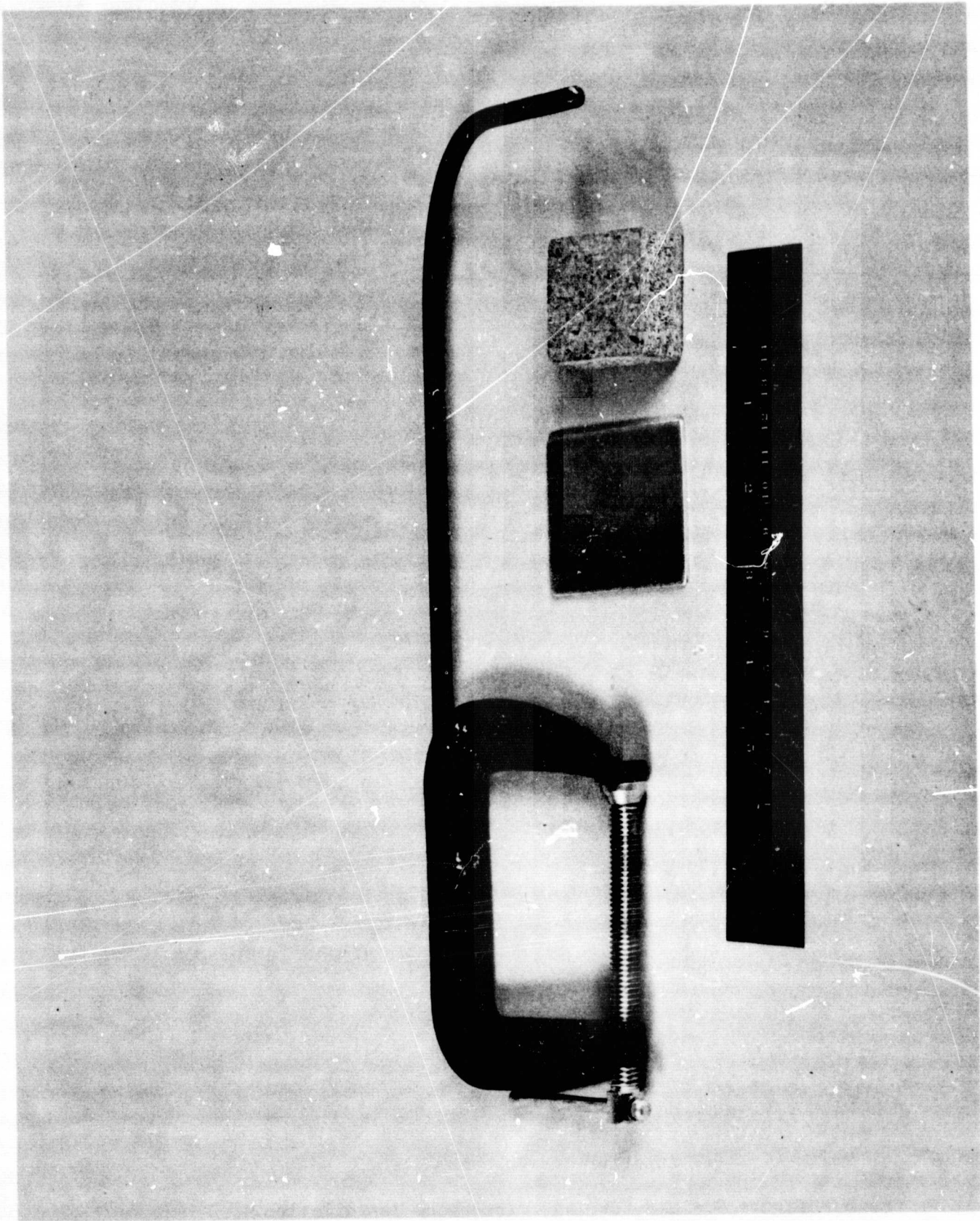
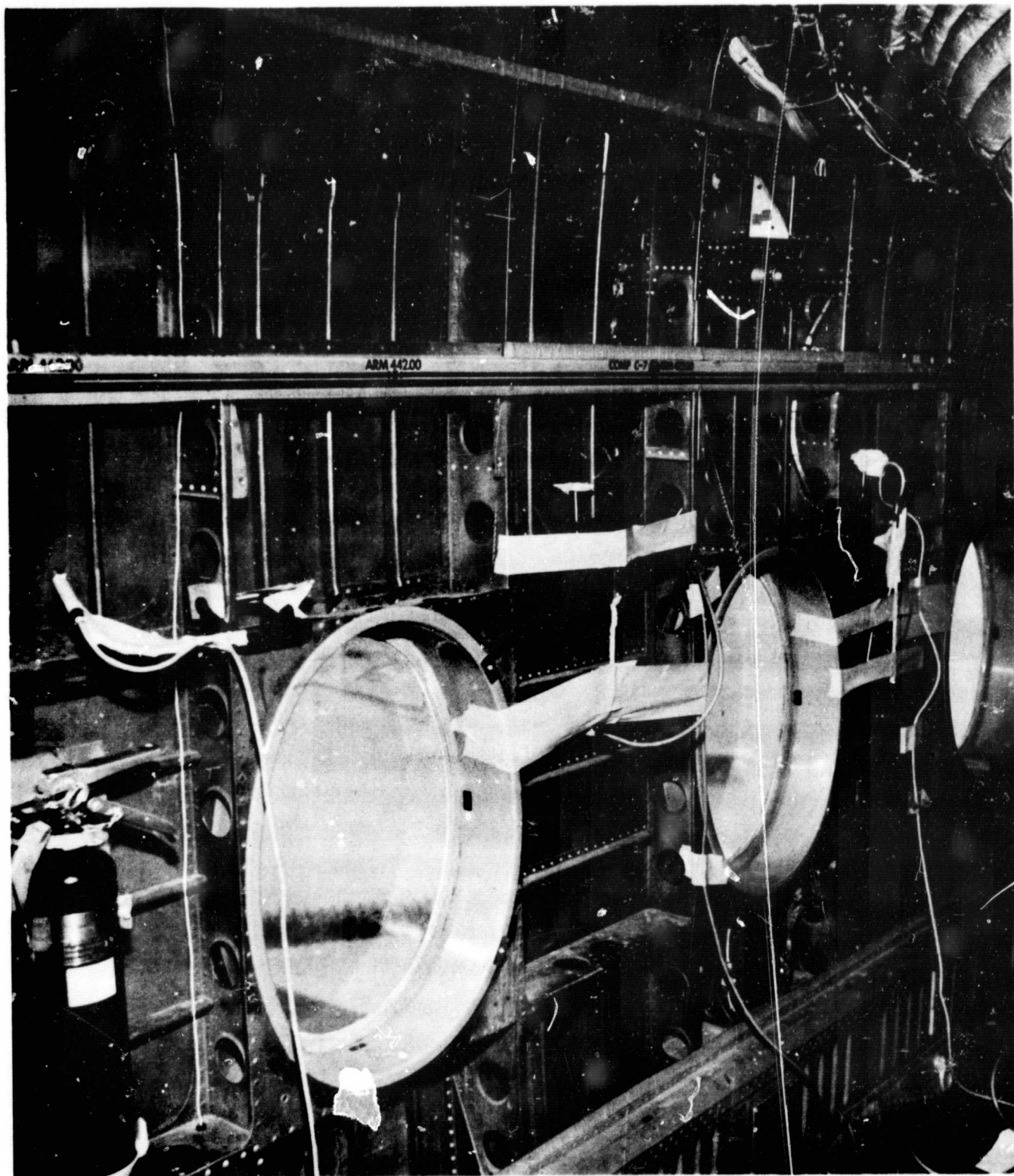


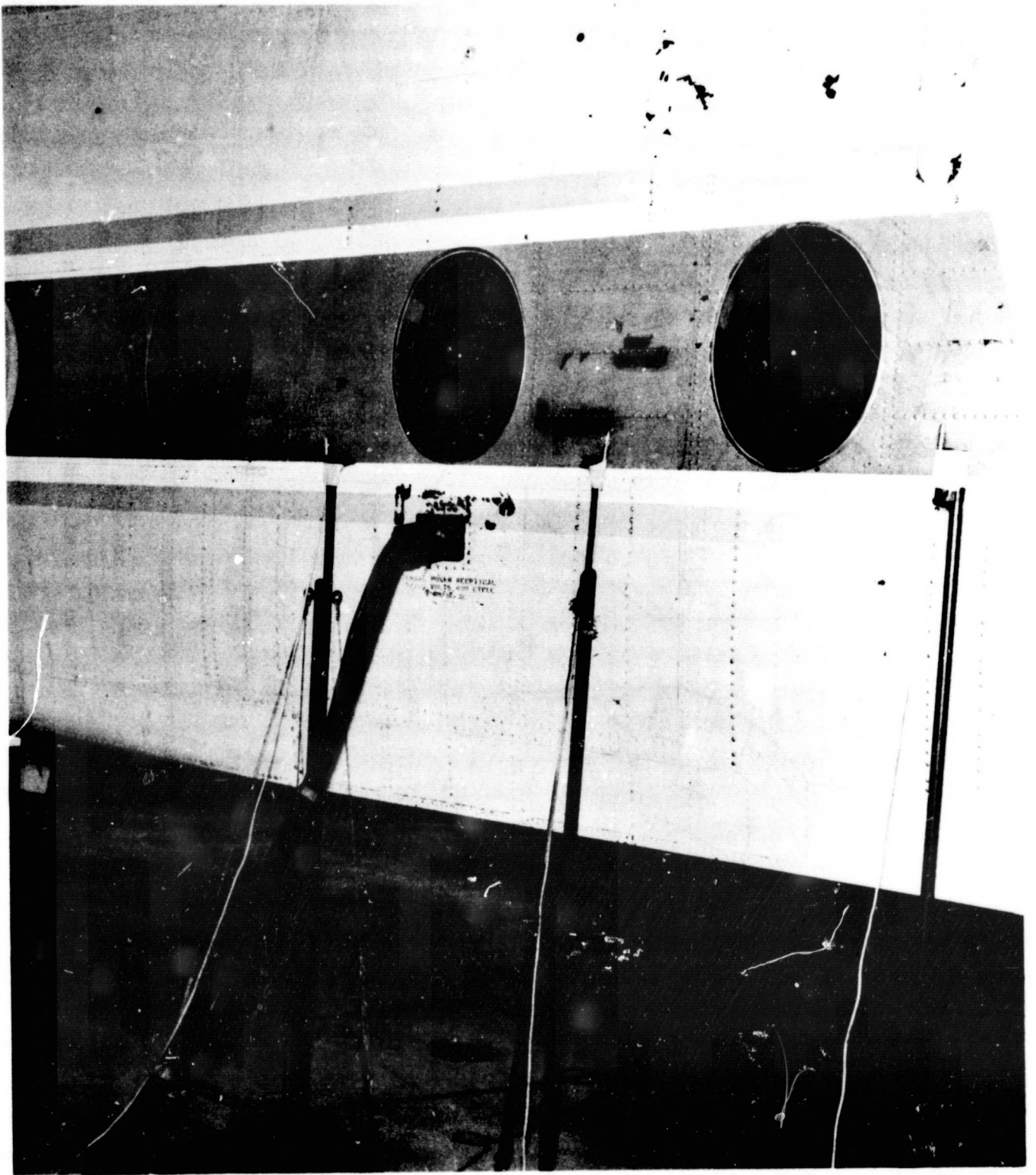
Figure 8.- "C" clamp fixture and pressure plates used to mount interior fuselage microphones 2-6.



(a) Interior microphones 2-4.

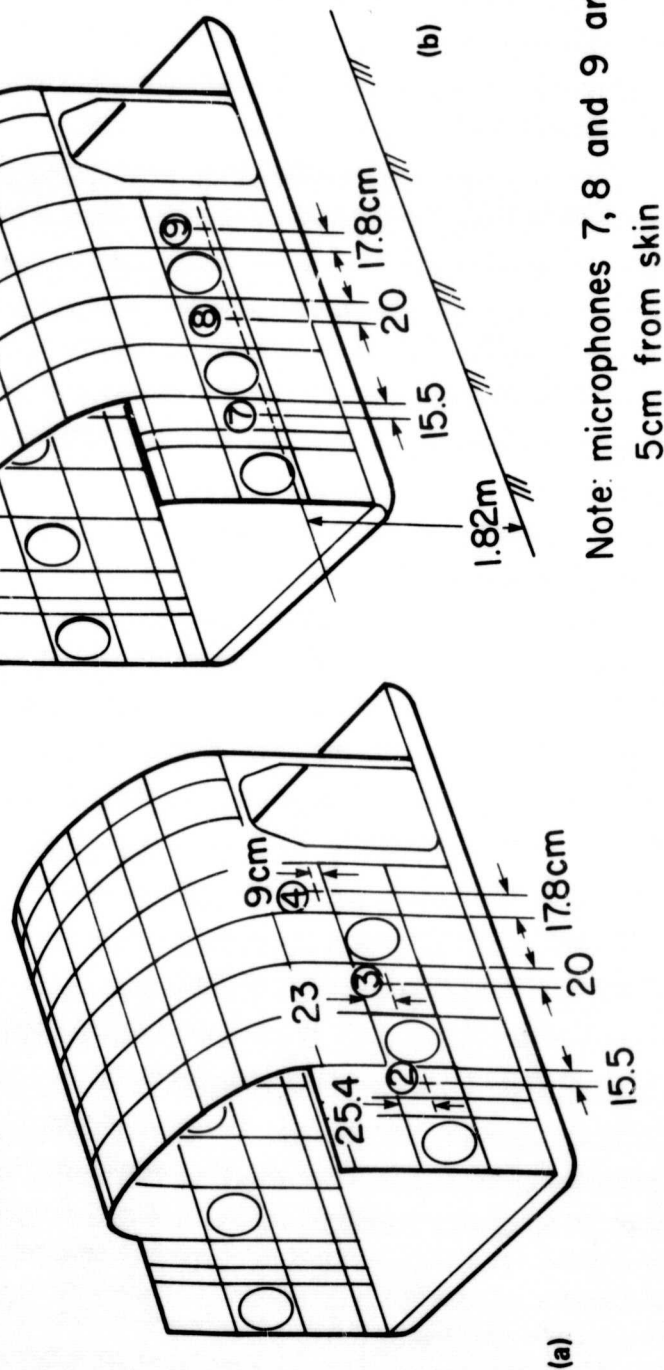
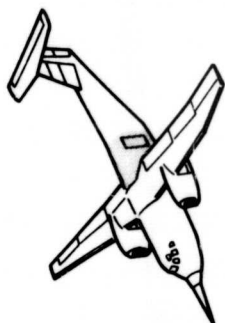
Figure 9.- Mid-fuselage microphone installation.

REPRODUCIBILITY OF THIS
COPY IS POOR



(b) Exterior microphones 7-9.

Figure 9.- Concluded.



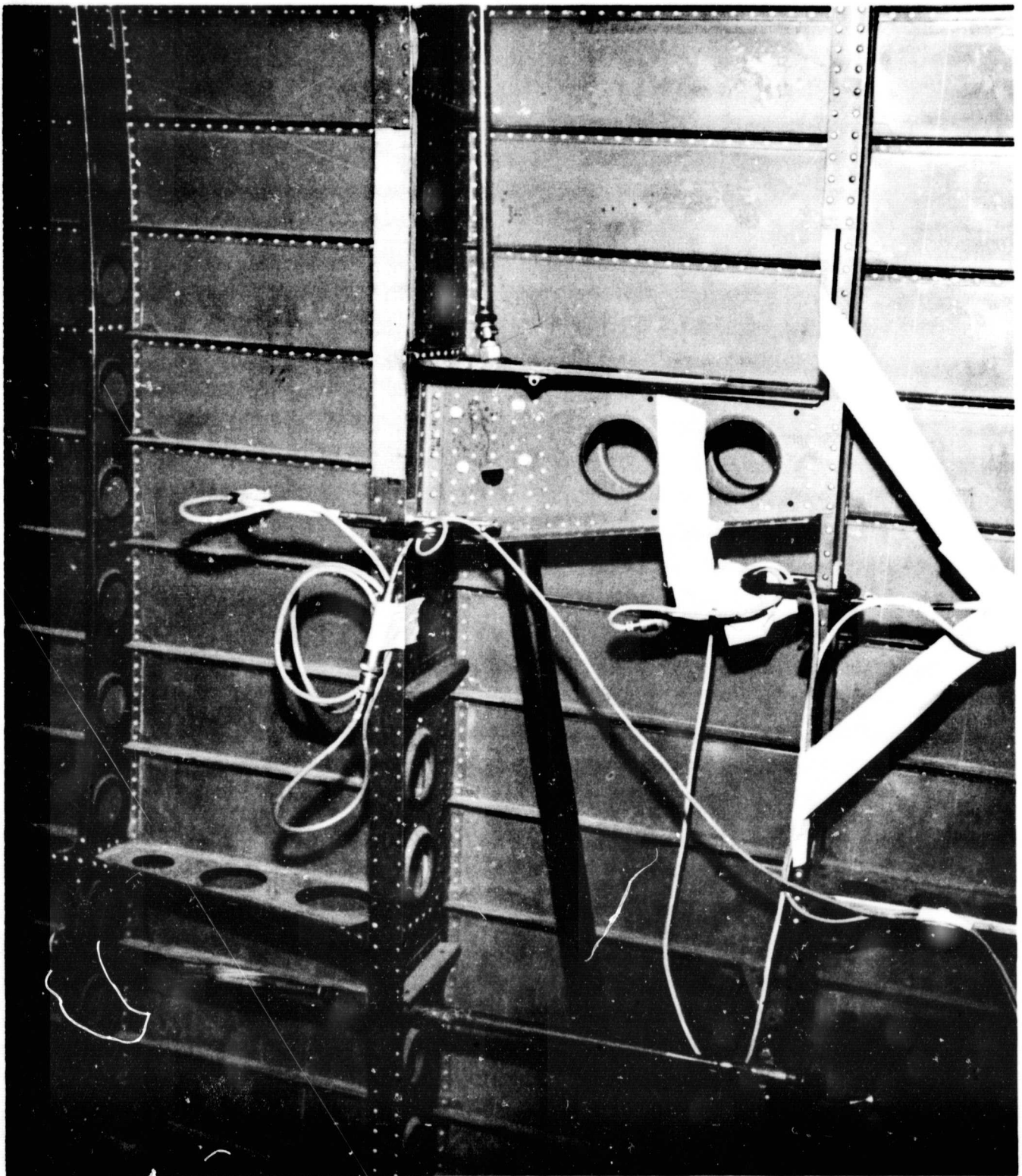
Note: microphones 7, 8 and 9 are 5cm from skin

Note: microphone 2 is 6cm from skin
microphone 3 and 4 are 2cm from skin

(a) Interior microphones 2-4.

(b) Exterior microphones 7-9.

Figure 10.— Dimensional layout of the mid-fuselage microphones.



(a) Interior microphones 5 and 6.

Figure 11.- Aft fuselage microphone installation.



(b) Exterior microphones 10 and 11.

Figure 11.- Concluded.

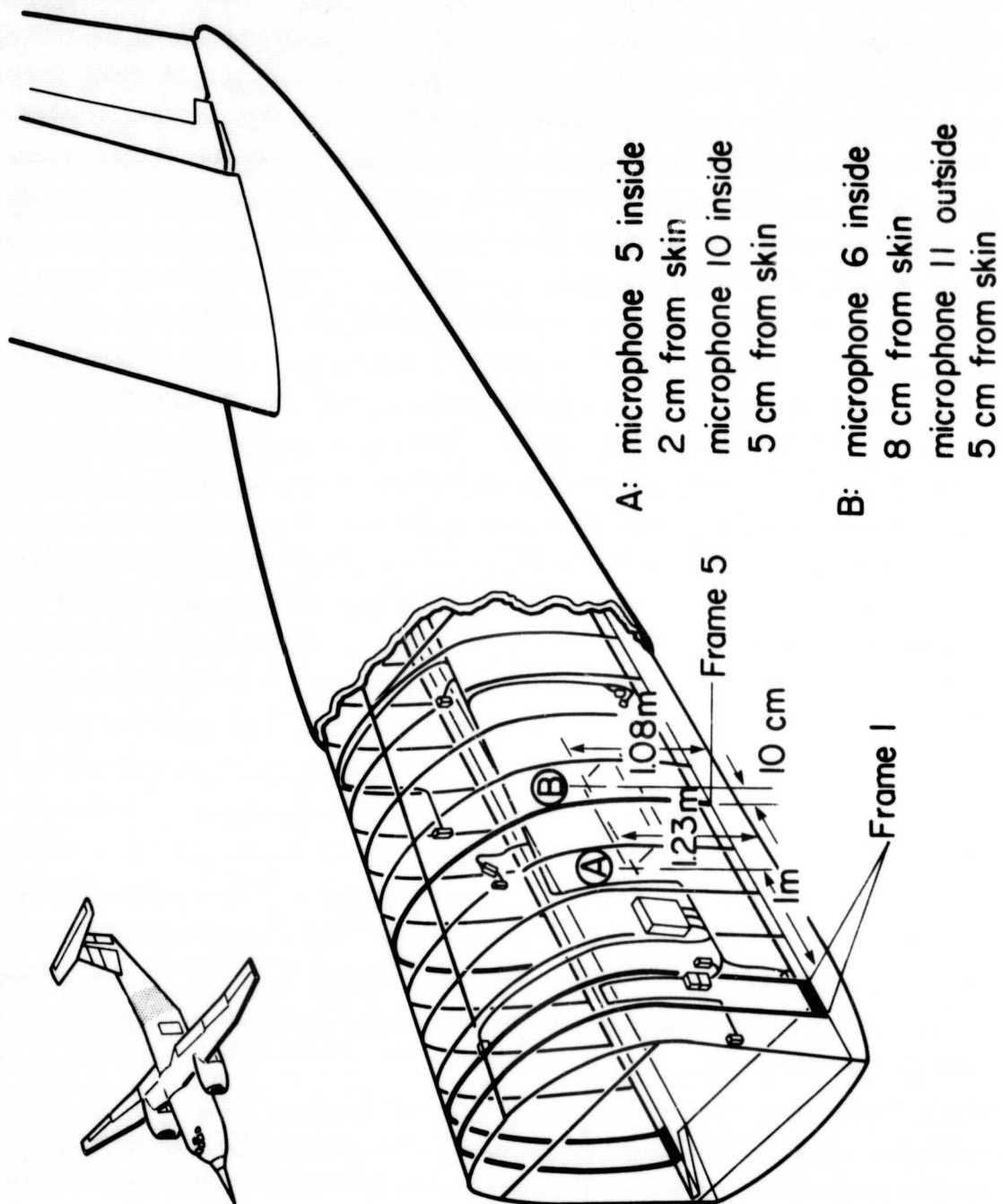


Figure 12.- Dimensional layout of aft microphones.

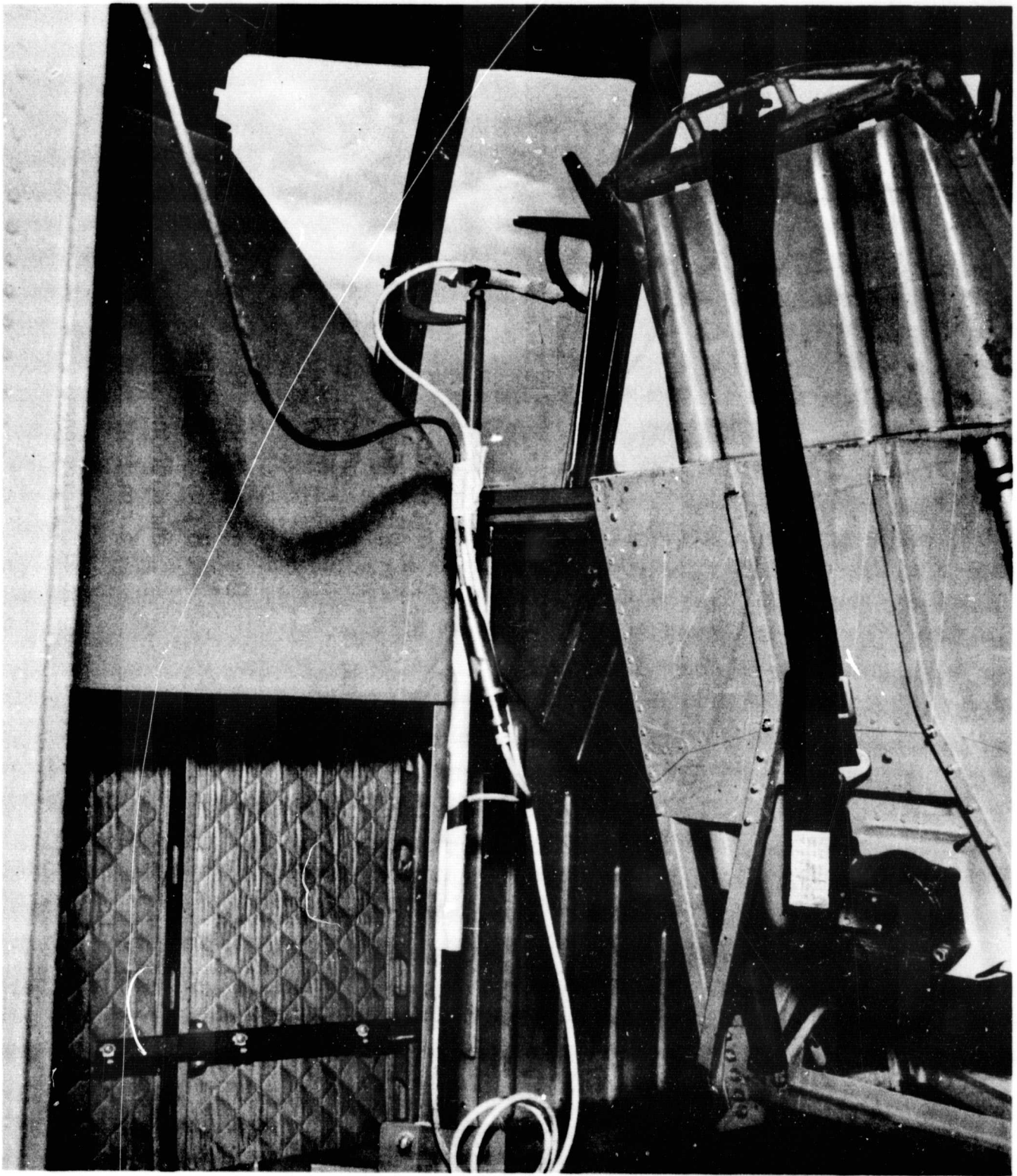


Figure 13.— Flight deck microphone installation.

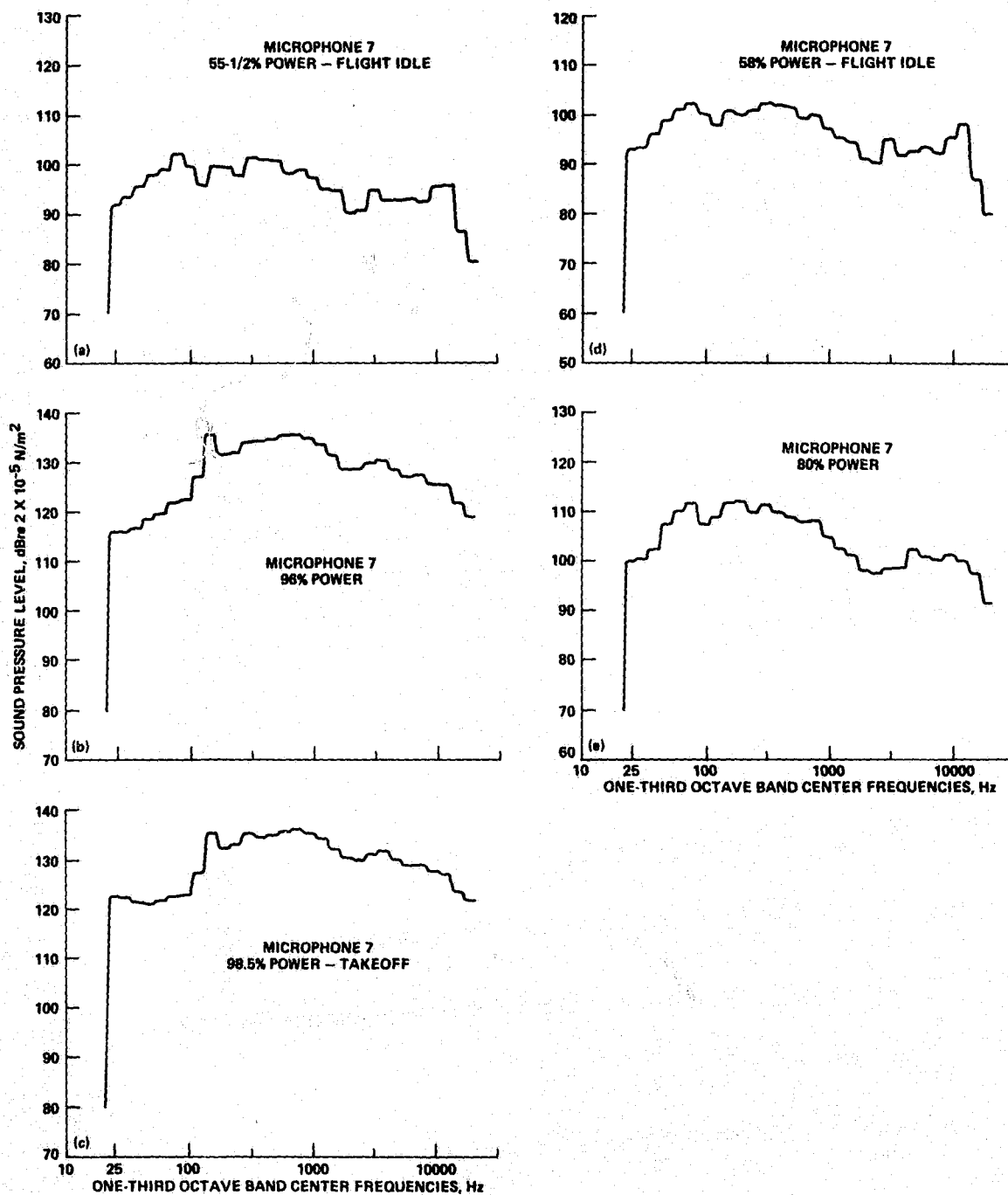


Figure 14.— One-third octave band sound pressure level at microphone 7.

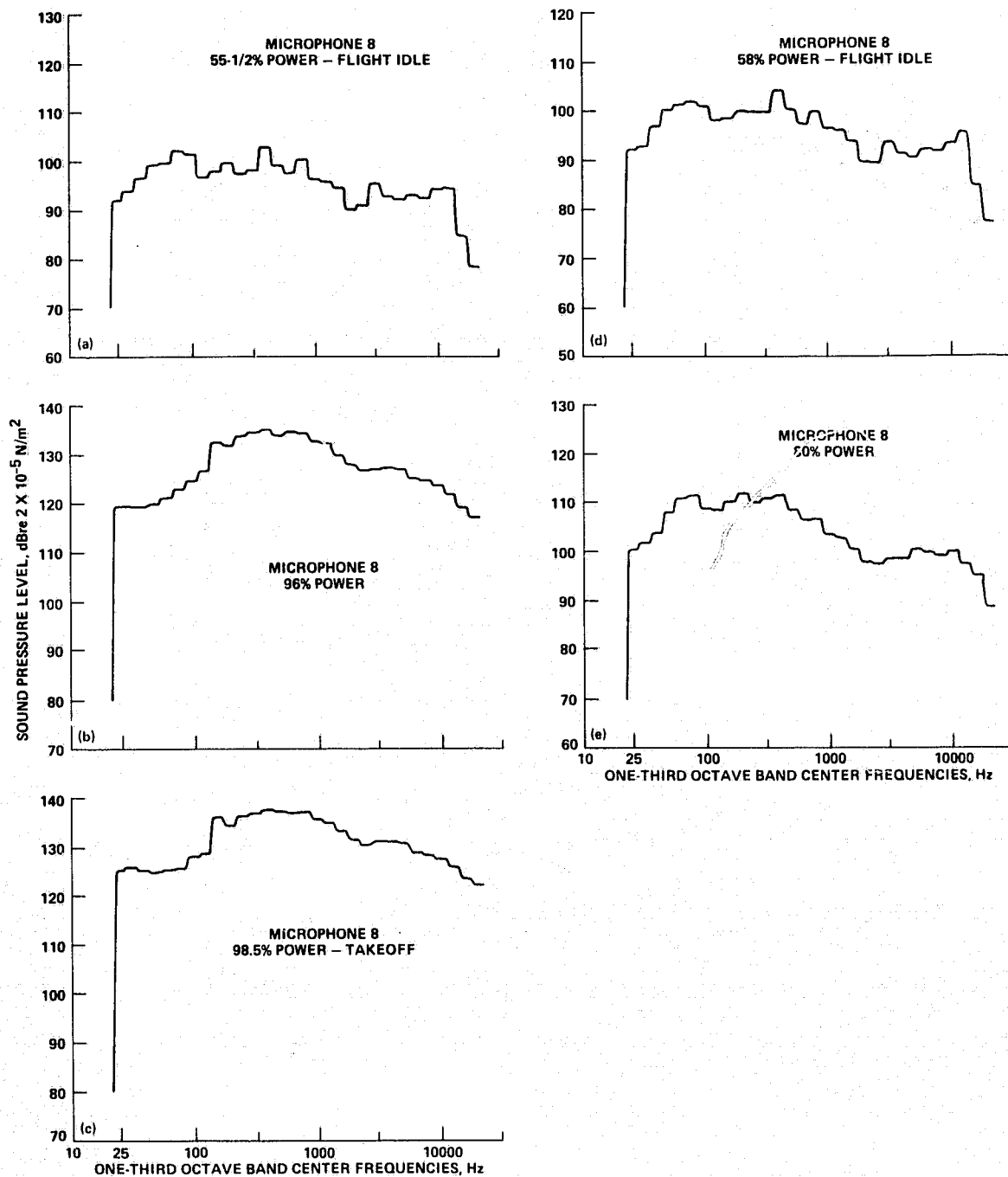


Figure 15.— One-third octave band sound pressure level at microphone 8.

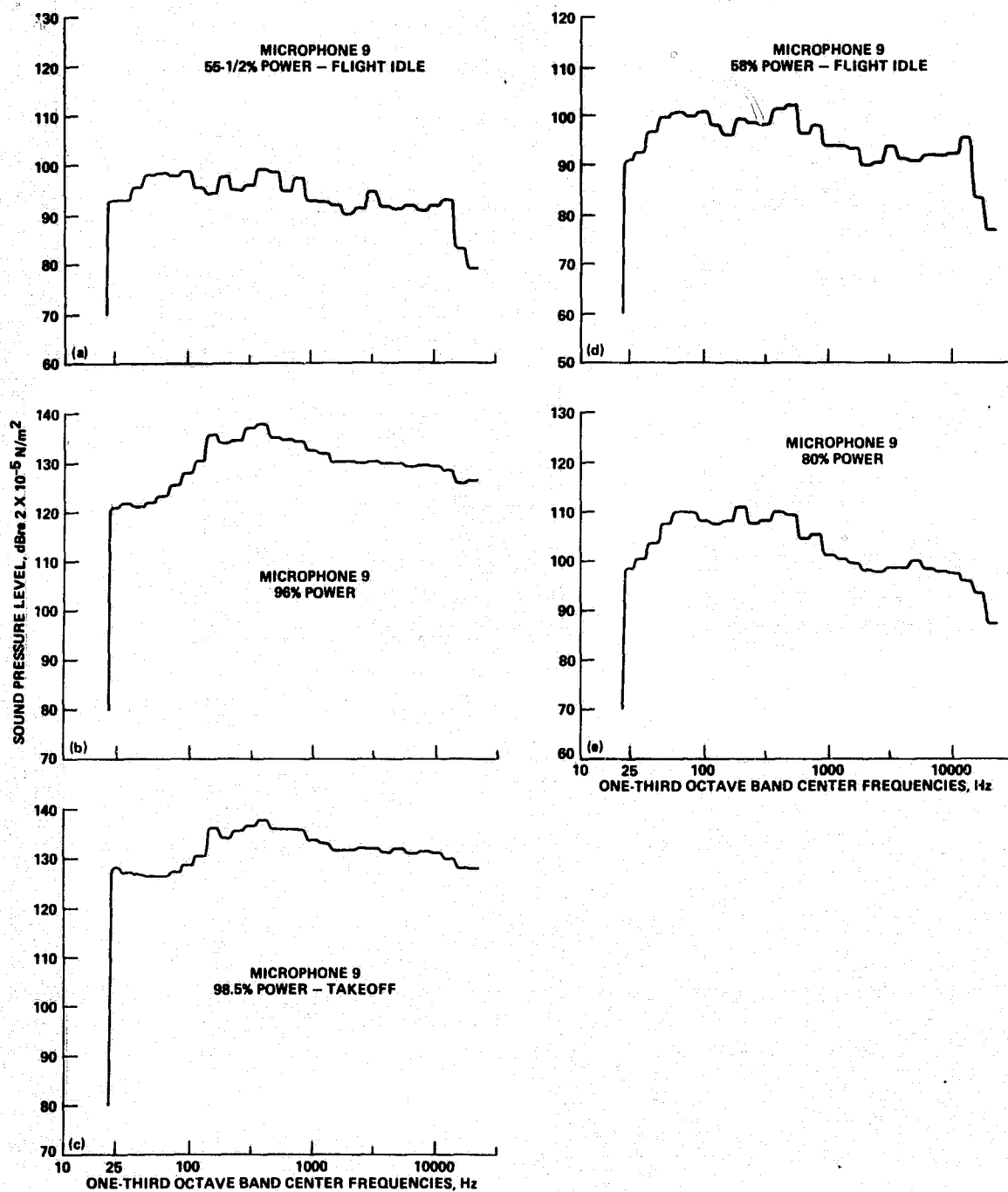


Figure 16.— One-third octave band sound pressure level at microphone 9.

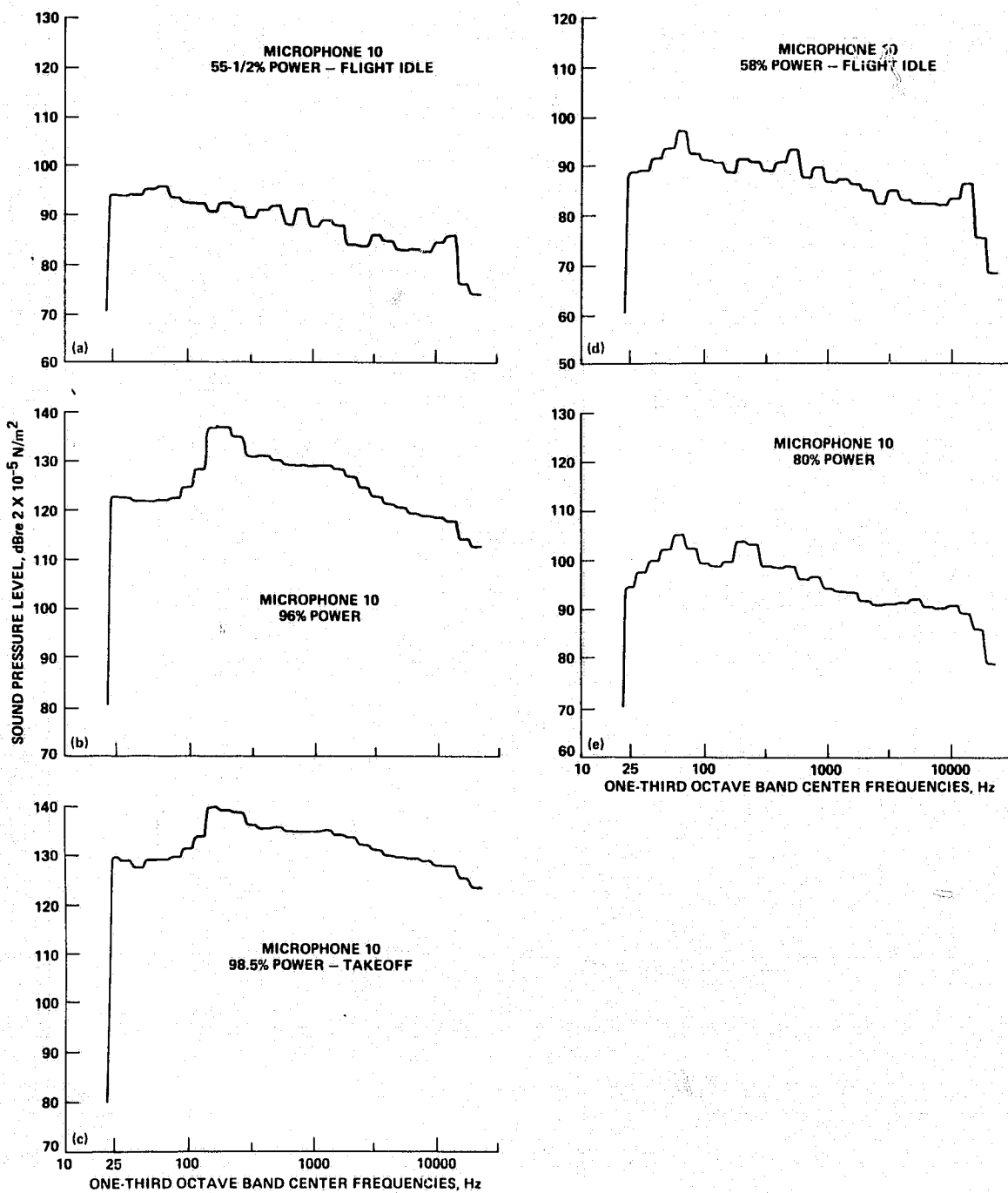


Figure 17.— One-third octave band sound pressure level at microphone 10.

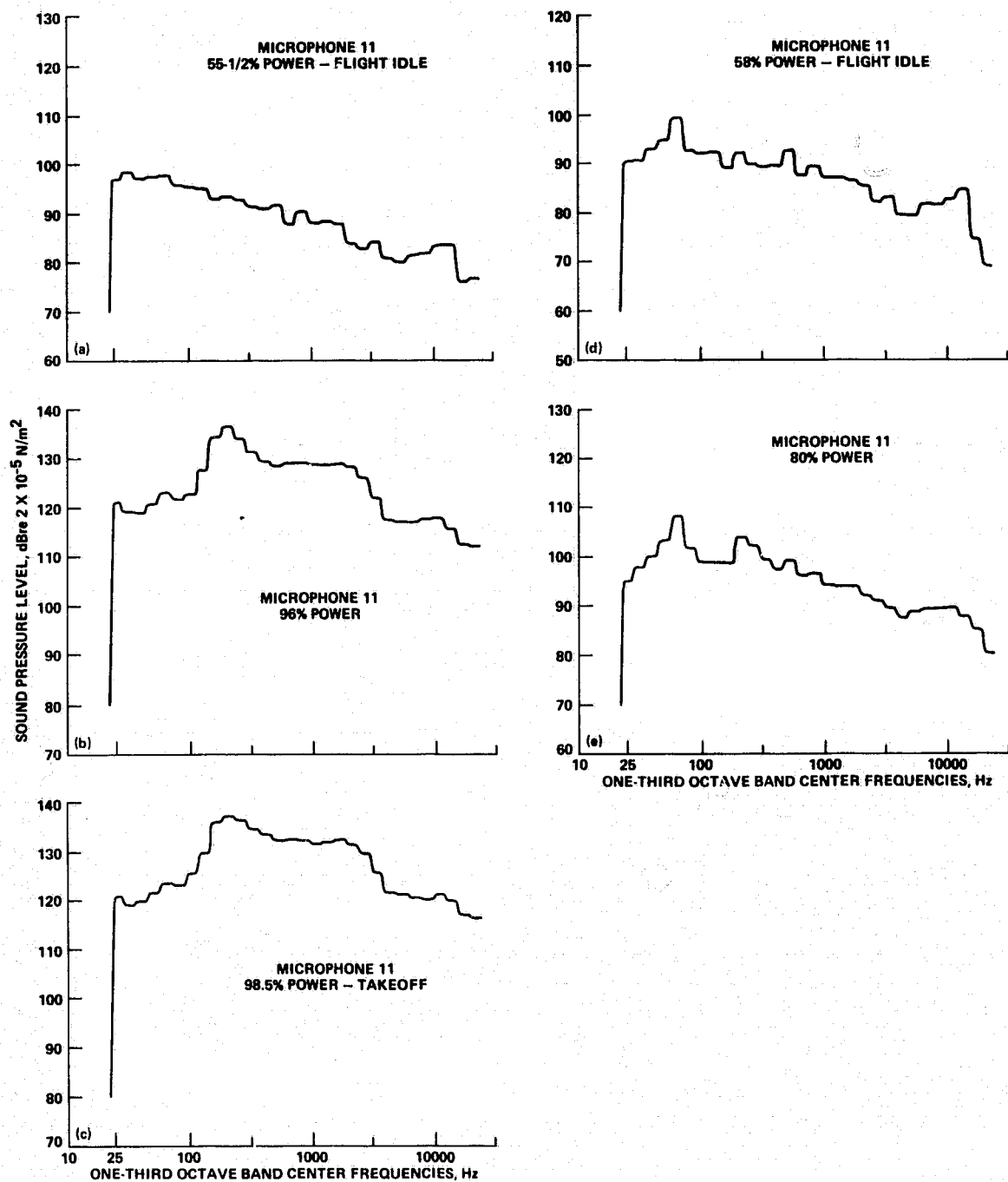


Figure 18.— One-third octave band sound pressure level at microphone 11.

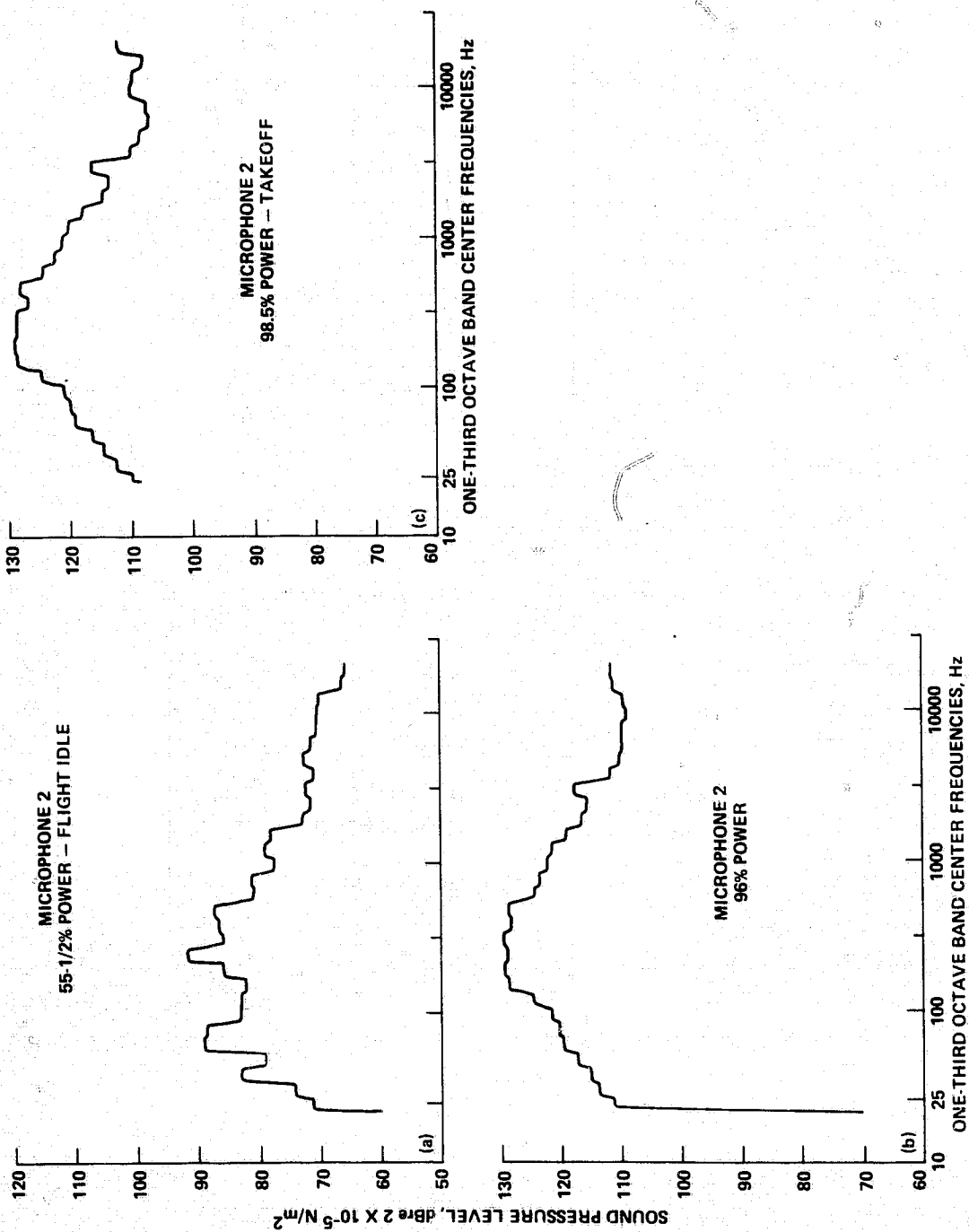


Figure 19.— One-third octave band sound pressure level at microphone 2.

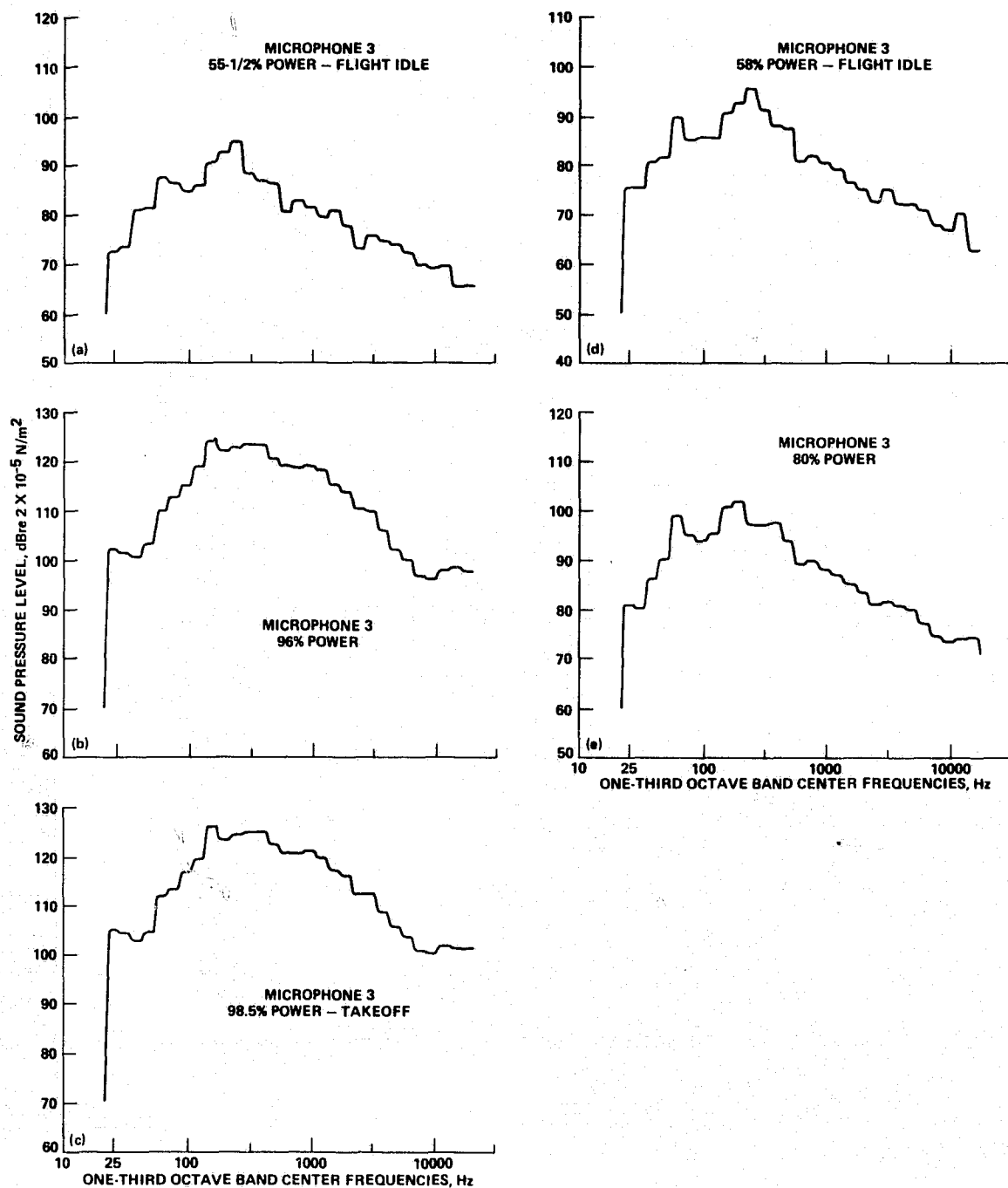


Figure 20.— One-third octave band sound pressure level at microphone 3.

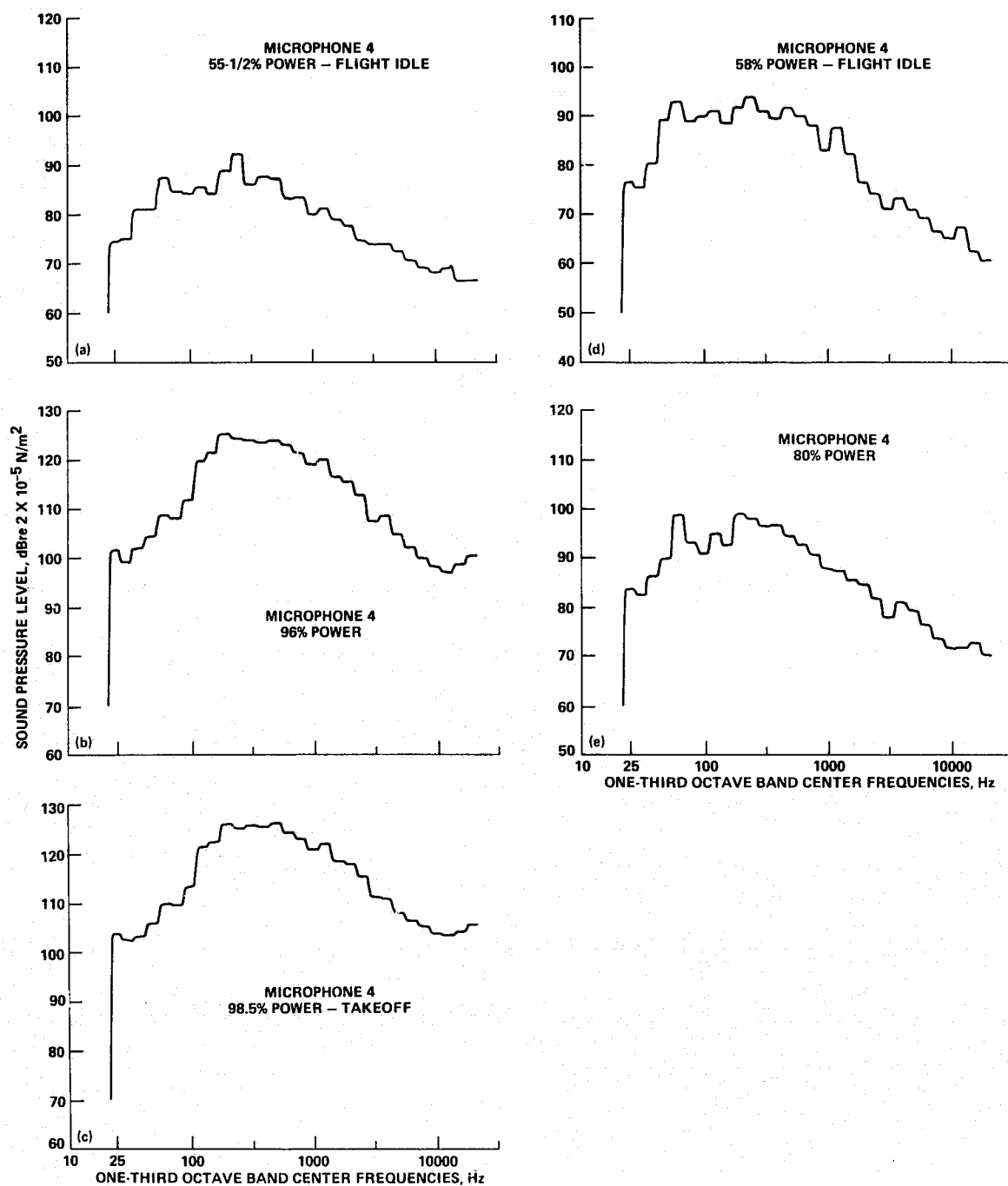


Figure 21.— One-third octave band sound pressure level at microphone 4.

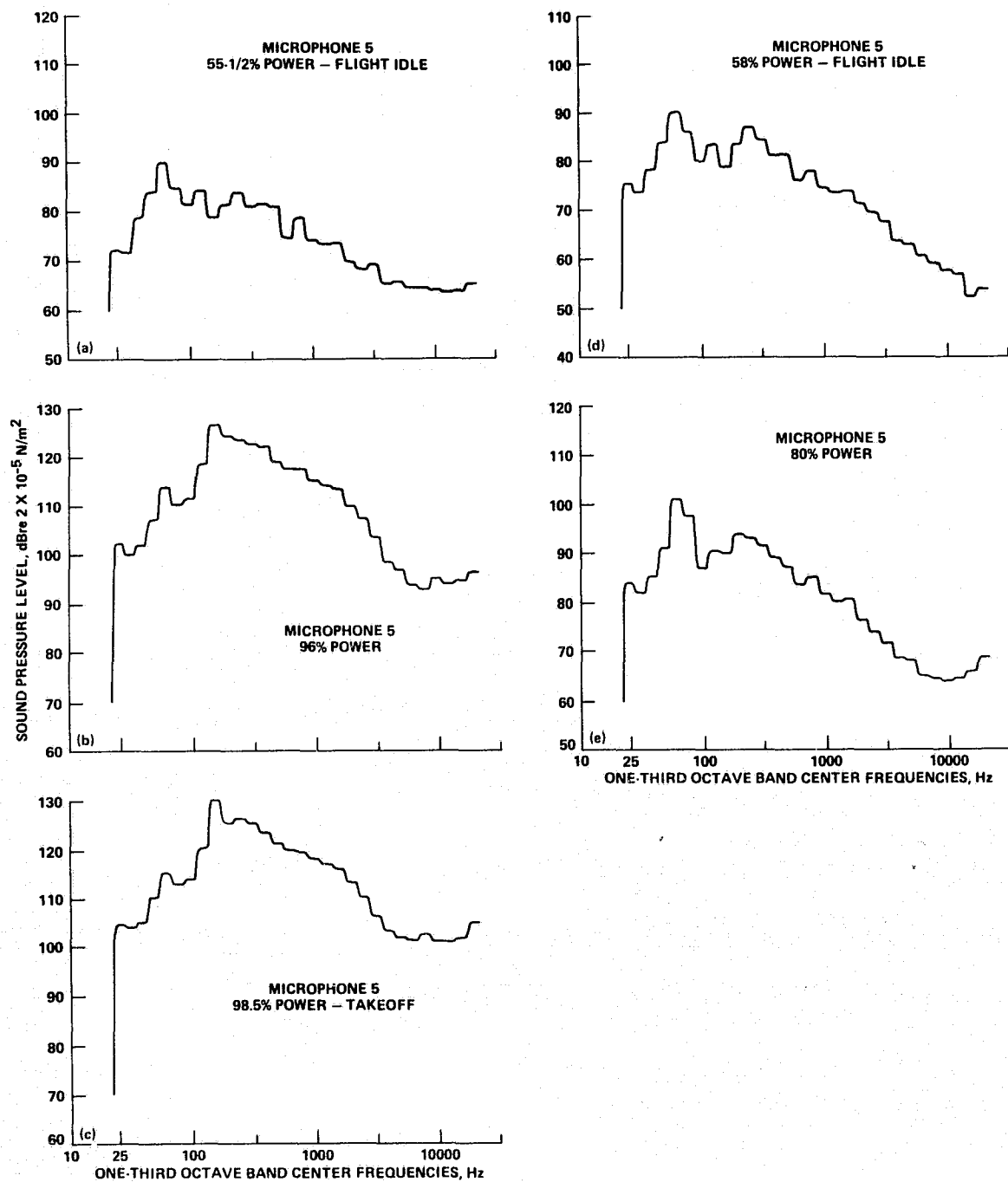


Figure 22.— One-third octave band sound pressure level at microphone 5.

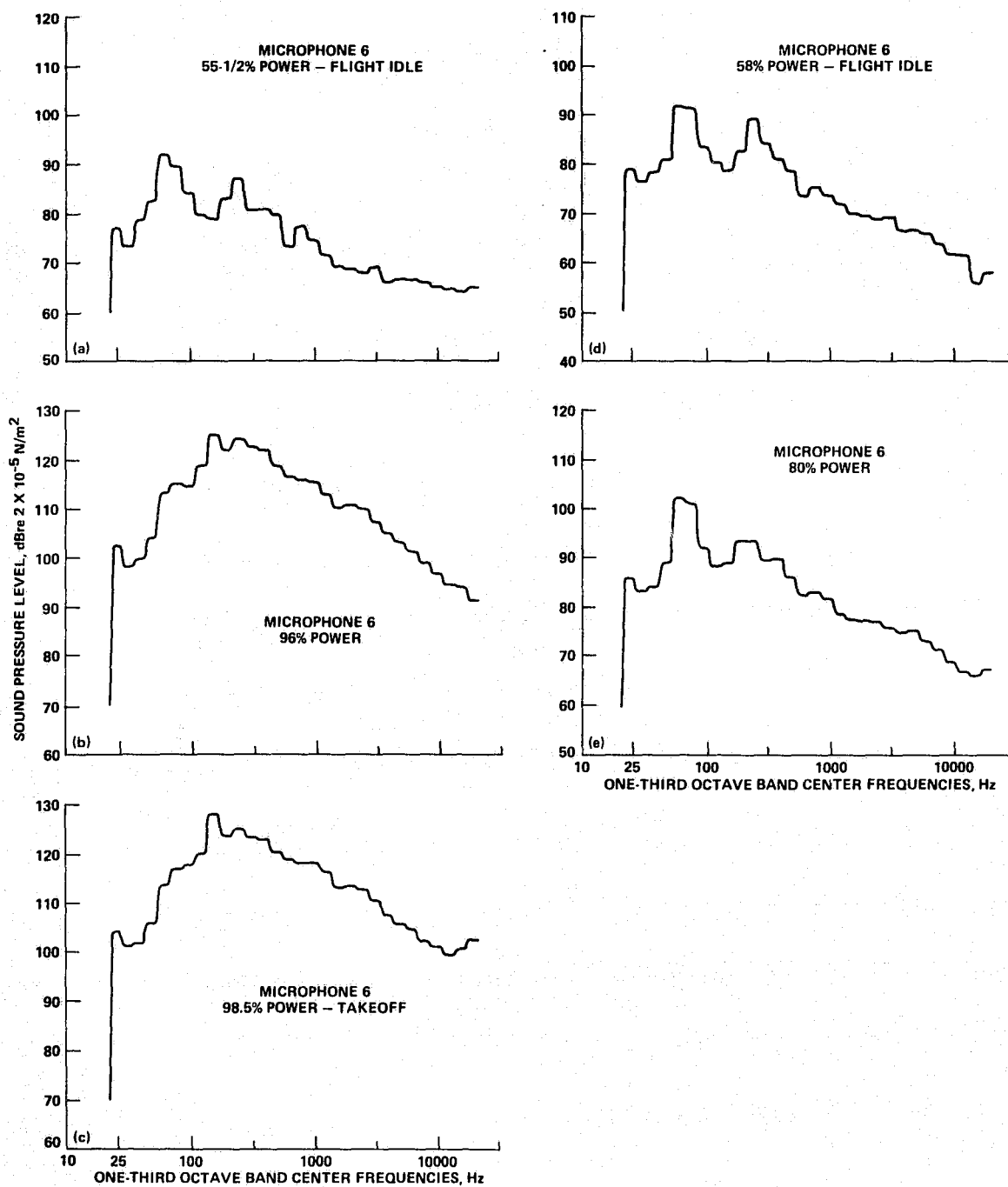


Figure 23.— One-third octave band sound pressure level at microphone 6.

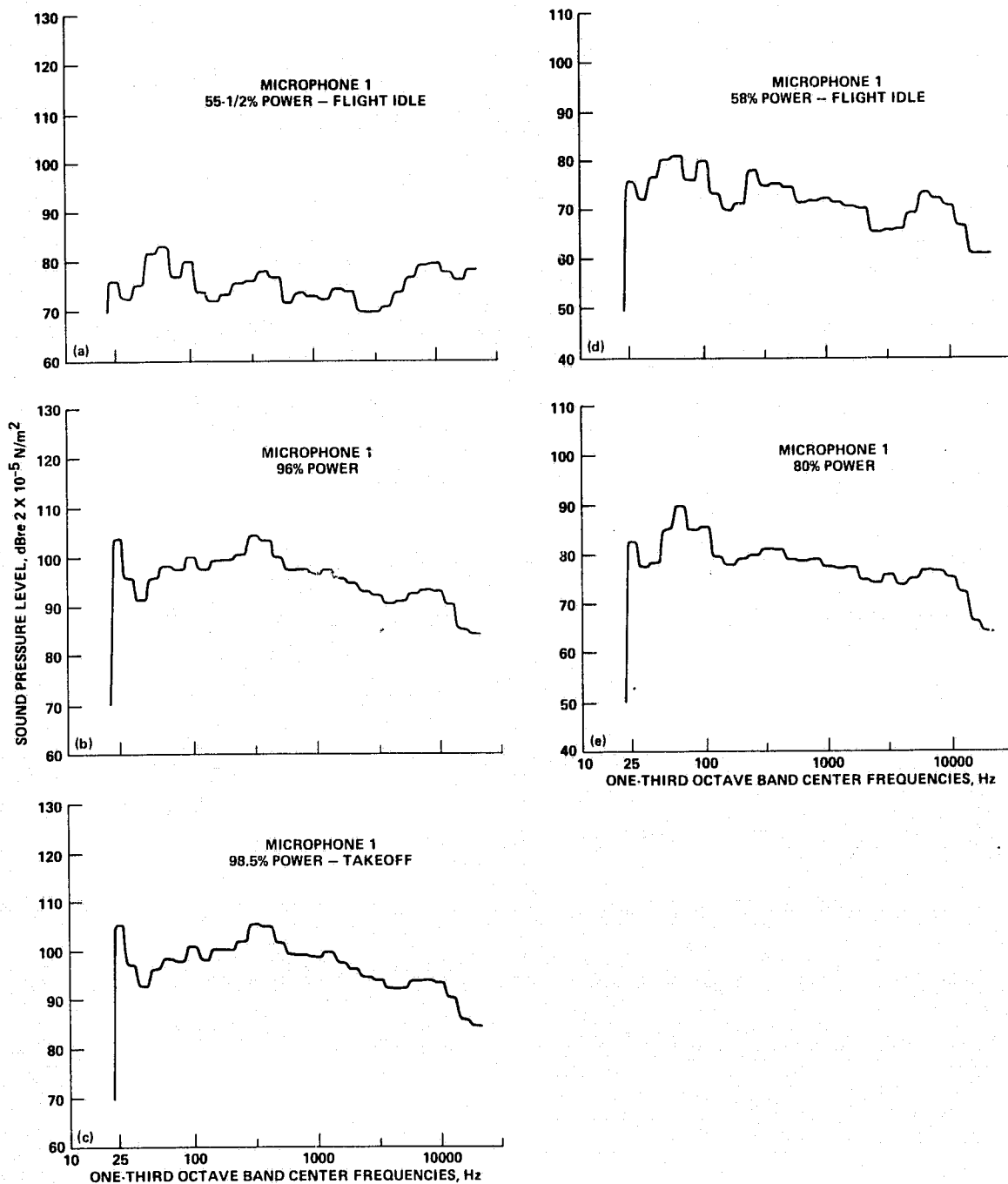
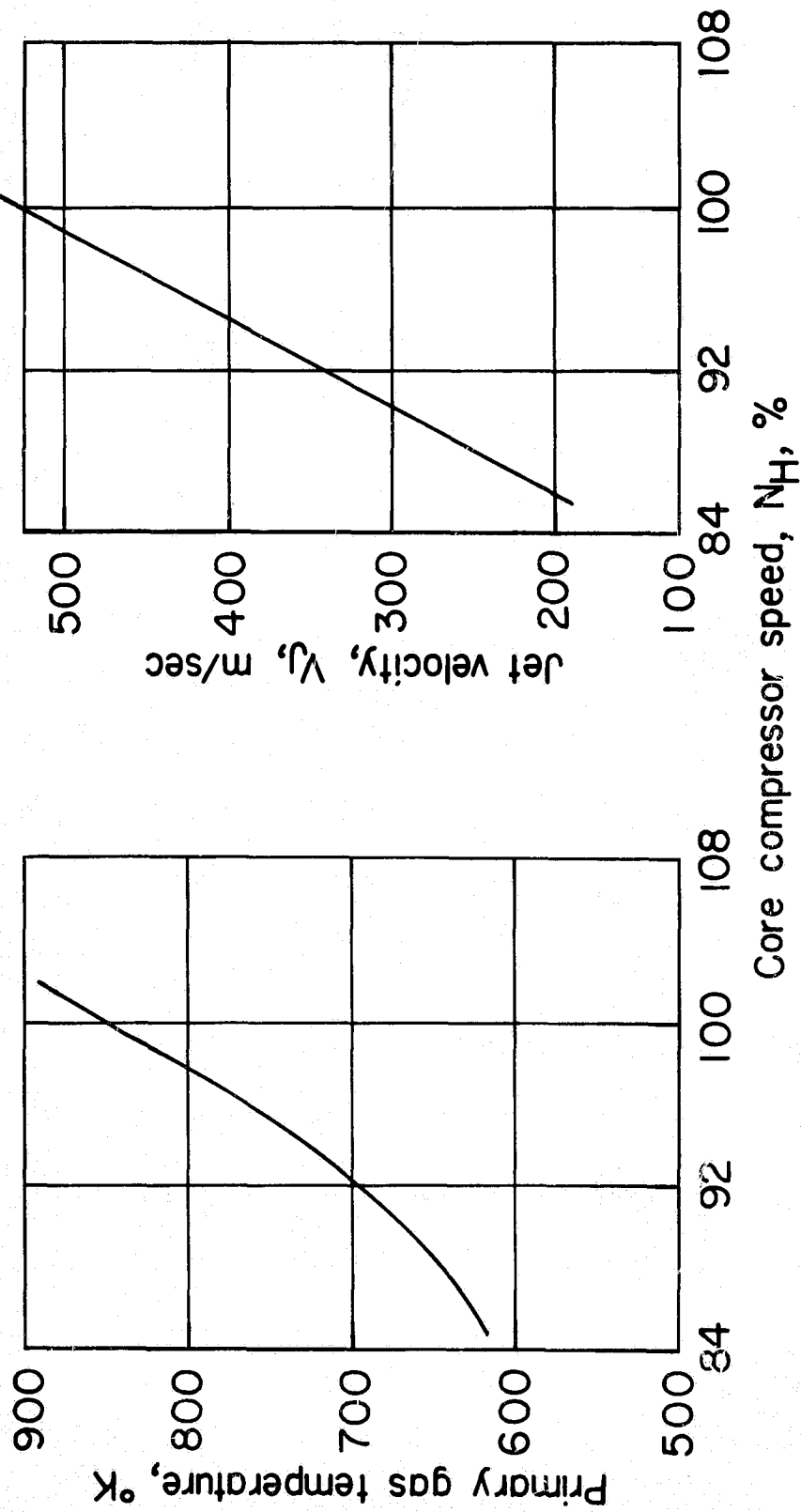


Figure 24.— One-third octave band sound pressure level on the flight deck at microphone 1.



(a) Primary jet gas temperature.

(b) Primary jet velocity.

Figure 25.— Physical characteristics of the primary jet.

Pertinent dimensions

$$\delta_F = 0.1 \text{ rad}$$

$$h_N = 1.07 \text{ cm}$$

$$l_T = 16.0 \text{ cm}$$

$$l'_Z = 18.8 \text{ cm}$$

$$Z = 5.8 \text{ cm}$$

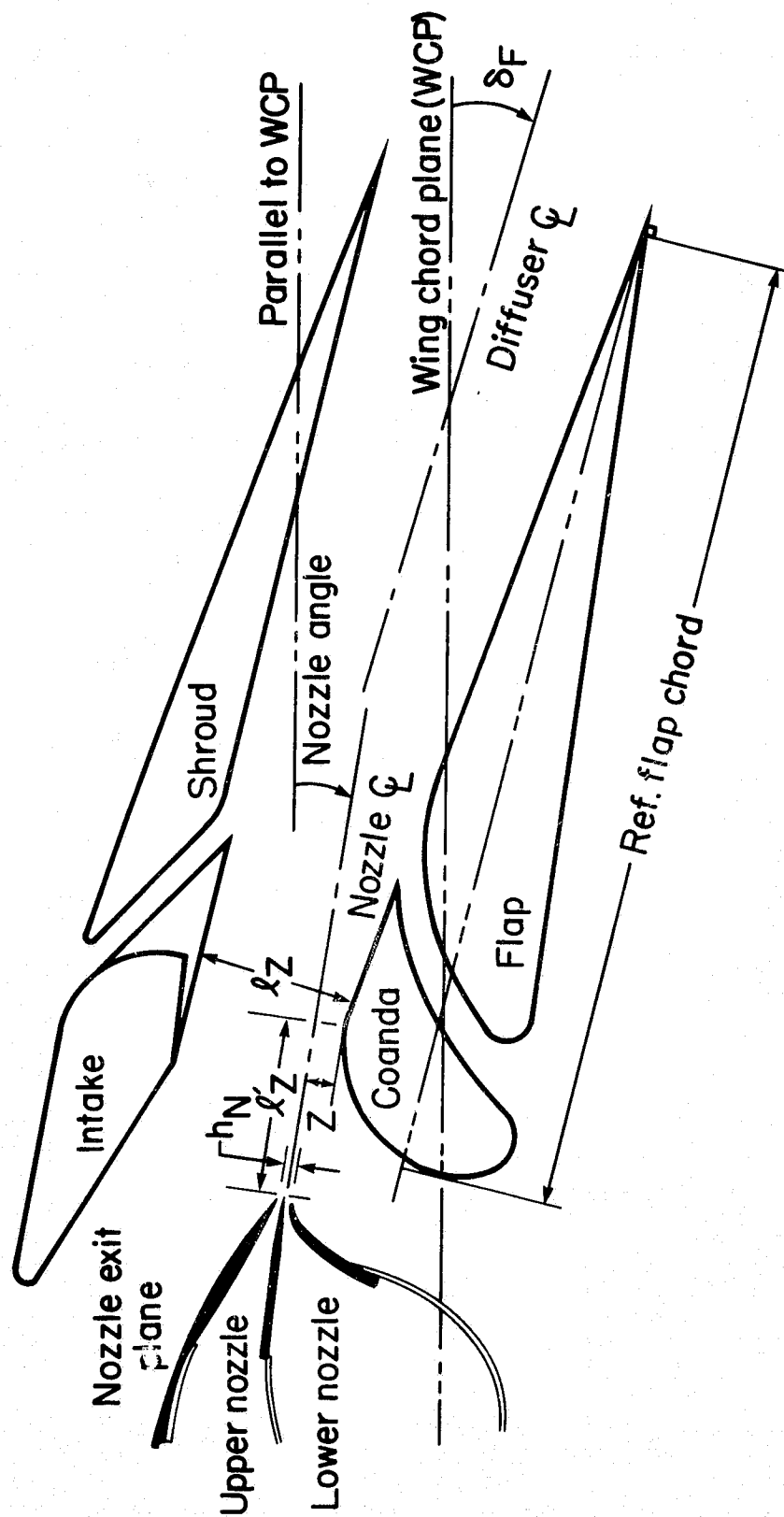
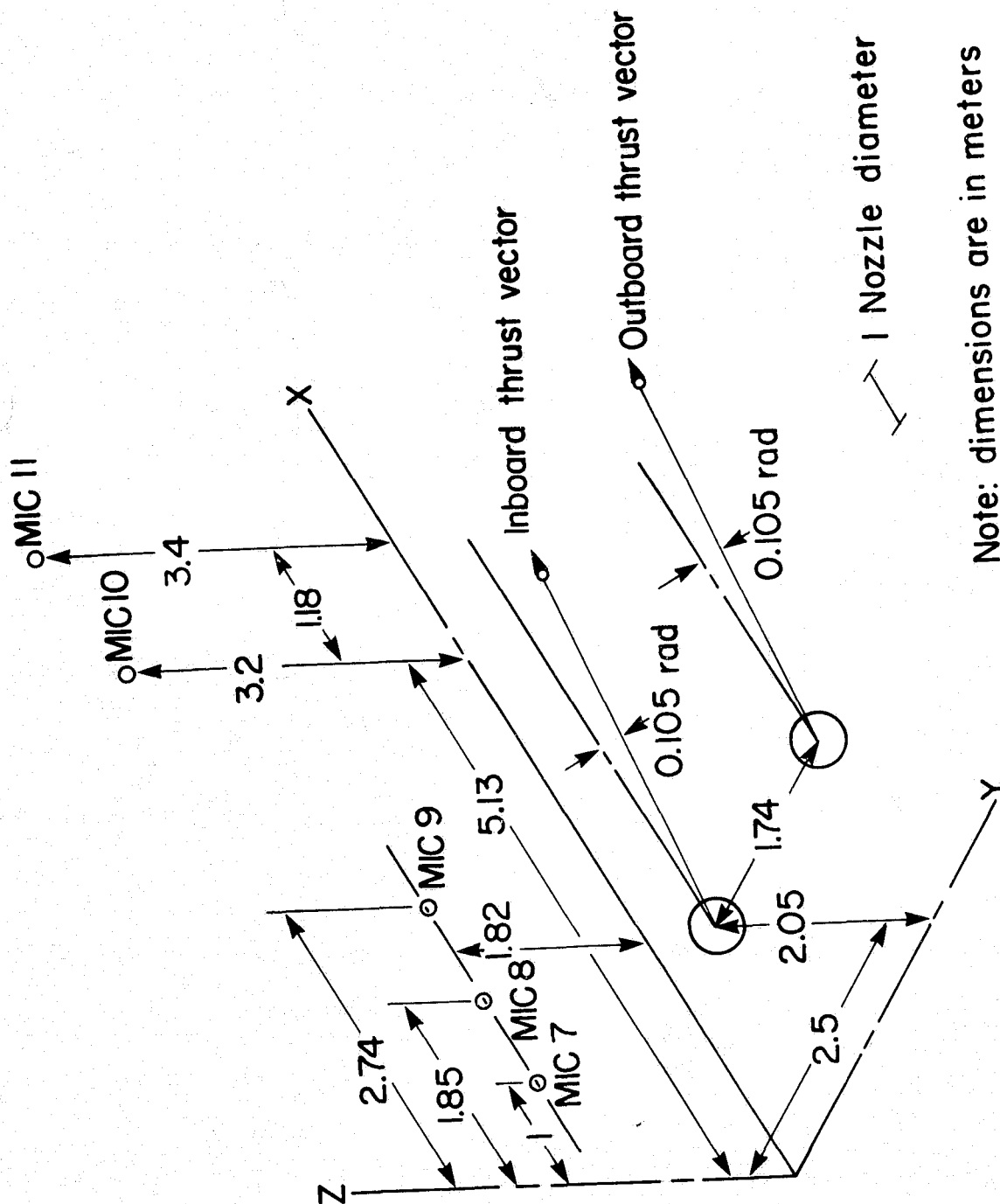


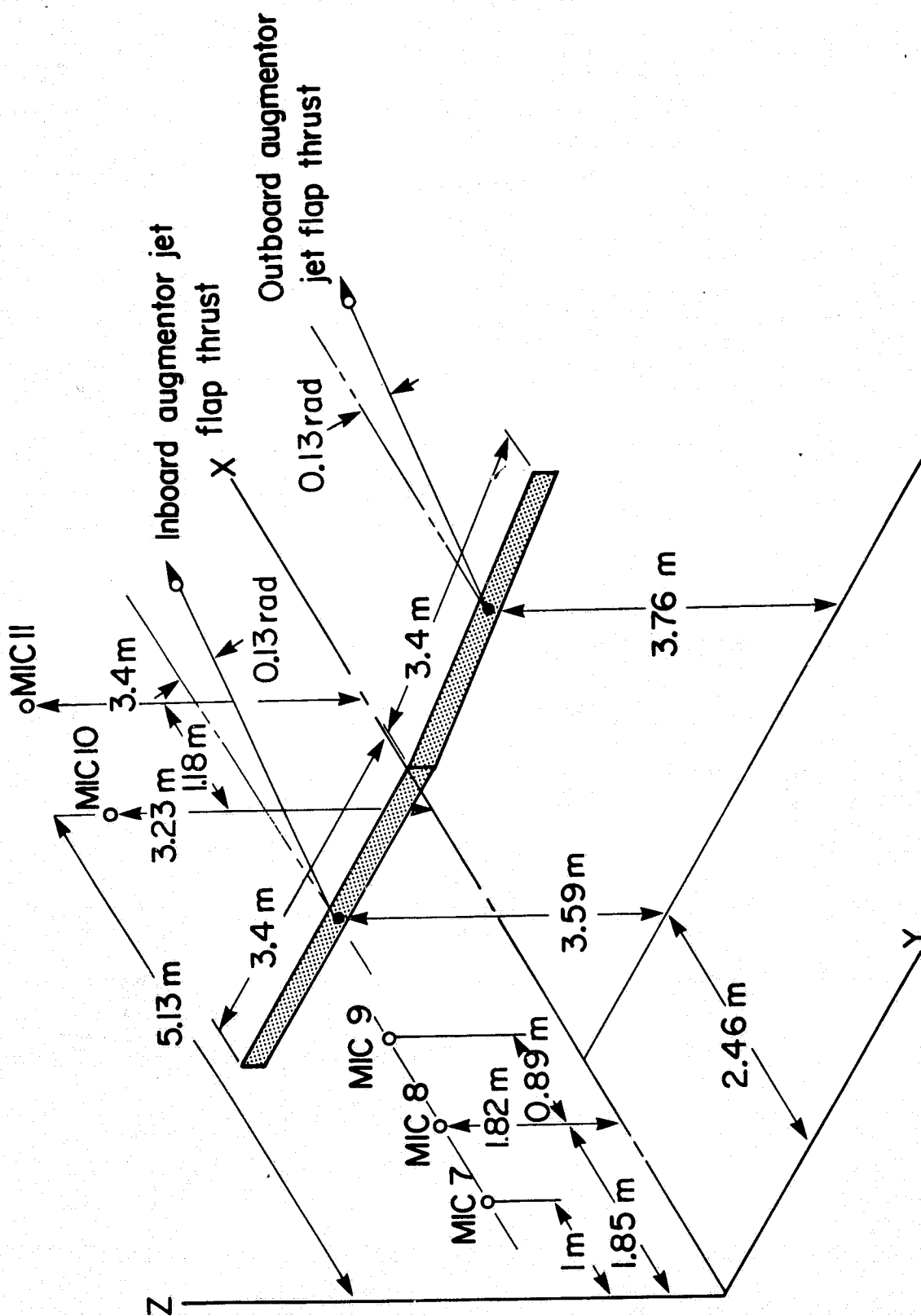
Figure 26.— Augmentor flap and ejector nozzle cross section.



Note: dimensions are in meters

(a) Primary jet noise source.

Figure 27.- Location of noise sources relative to the external field microphone location.



(b) Augmentor flap noise source.

Figure 27.- Concluded.

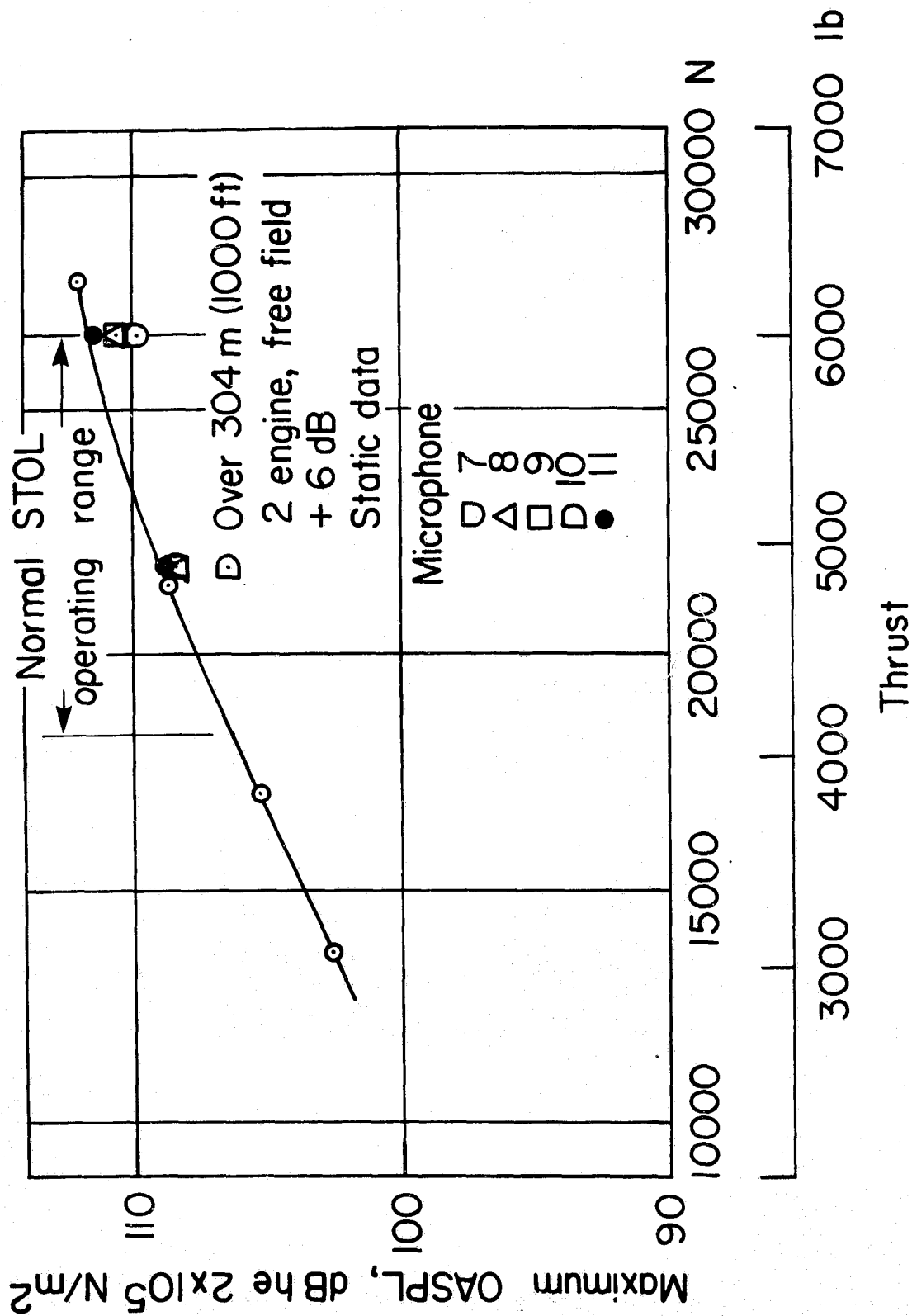


Figure 28.— Overall sound pressure level correlation with hot thrust level.
Data from microphones 7-11 extrapolated to 1000 m and compared
with OASPI curve from figure 10 of reference 3.